Article

Current Biology

Transcription activator-like effector protects bacterial endosymbionts from entrapment within fungal hyphae

Highlights

- TAL effectors circumvent host defense in a bacterial-fungal endosymbiosis
- Microfluidics reveal trapping of effector-deficient bacteria in fungal side hyphae
- Unprecedented case of septa formation in Mucoromycota fungi
- Endosymbionts rely on TAL effectors to aid their intracellular lifestyle

Authors

Ingrid Richter, Philipp Wein, Zerrin Uzum, ..., Iuliia Ferling, Falk Hillmann, Christian Hertweck

Correspondence

christian.hertweck@leibniz-hki.de

In brief

Richter et al. show that a transcription activator-like (TAL) effector of bacteria living within a phytopathogenic fungus is an essential symbiosis factor. Microfluidics and live imaging reveal septa formation in fungal side hyphae, which traps TAL effector-deficient bacteria, leading to reduced survival.

Richter et al., 2023, Current Biology *33*, 2646–2656
July 10, 2023
https://doi.org/10.1016/j.cub.2023.05.028

CellPress

CellPress
OPEN ACCESS

Current Biology

Article

Transcription activator-like effector protects bacterial endosymbionts from entrapment within fungal hyphae

Ingrid Richter,[1,5,8,9] Philipp Wein,[1,8] Zerrin Uzum,[1] Claire E. Stanley,[2] Jana Krabbe,[1,8] Evelyn M. Molloy,[1,8] Nadine Moebius,[1] Iuliia Ferling,[3] Falk Hillmann,[3,6] and Christian Hertweck[1,4,7,8,9,10,*]

[1]Department of Biomolecular Chemistry, Leibniz Institute for Natural Product Research and Infection Biology, HKI, Beutenbergstr. 11a, 07745 Jena, Germany
[2]Department of Bioengineering, Imperial College, South Kensington, London SW7 2AZ, UK
[3]Junior Research Group Evolution of Microbial Interactions, Leibniz Institute for Natural Product Research and Infection Biology, Beutenbergstr. 11a, 07745 Jena, Germany
[4]Institute of Microbiology, Faculty of Biological Sciences, Friedrich Schiller University Jena, 07743 Jena, Germany
[5]Twitter: @Funbiosis2017
[6]Twitter: @HillmannLab
[7]Twitter: @Hertweck_Lab
[8]Twitter: @LeibnizHKI
[9]Twitter: @chembiosys_jena
[10]Lead contact
*Correspondence: christian.hertweck@leibniz-hki.de
https://doi.org/10.1016/j.cub.2023.05.028

SUMMARY

As an endosymbiont of the ecologically and medically relevant fungus *Rhizopus microsporus*, the toxin-producing bacterium *Mycetohabitans rhizoxinica* faces myriad challenges, such as evading the host's defense mechanisms. However, the bacterial effector(s) that facilitate the remarkable ability of *M. rhizoxinica* to freely migrate within fungal hyphae have thus far remained unknown. Here, we show that a transcription activator-like (TAL) effector released by endobacteria is an essential symbiosis factor. By combining microfluidics with fluorescence microscopy, we observed enrichment of TAL-deficient *M. rhizoxinica* in side hyphae. High-resolution live imaging showed the formation of septa at the base of infected hyphae, leading to the entrapment of endobacteria. Using a LIVE/DEAD stain, we demonstrate that the intracellular survival of trapped TAL-deficient bacteria is significantly reduced compared with wild-type *M. rhizoxinica*, indicative of a protective host response in the absence of TAL proteins. Subversion of host defense in TAL-competent endobacteria represents an unprecedented function of TAL effectors. Our data illustrate an unusual survival strategy of endosymbionts in the host and provide deeper insights into the dynamic interactions between bacteria and eukaryotes.

INTRODUCTION

Endosymbiosis, a symbiotic relationship in which a microbial partner lives within its host, has led to some of the major evolutionary transitions, e.g., the formation of mitochondria and chloroplasts from internalized prokaryotes.[1] Endosymbiosis represents the most intimate contact between interacting partners and, in many cases, has reached a point of strict dependency on the symbiotic partner after millions of years of evolution.[2] Such obligate relationships are frequently observed between endofungal bacteria and Mucoromycota fungi.[3,4]

One pertinent example is the intriguing endosymbiosis between the Mucoromycota fungus *Rhizopus microsporus* and its bacterial symbiont, *Mycetohabitans rhizoxinica*.[5–7] *R. microsporus* is the causative agent of rice seedling blight, a disease that causes severe crop losses in agriculture in Asia.[8] The symbiont resides within the fungal hypha, where it produces the highly potent phytotoxin rhizoxin, which is partly tailored by the fungus before being excreted to efficiently stall plant cell division.[9] The *R. microsporus-M. rhizoxinica* symbiosis is unique not only in being a phytotoxin-producing alliance but also because host reproduction through spores is reliant on the presence of endobacteria (Figure 1A). If cured of its endosymbionts by antibiotic treatment, *R. microsporus* is unable to reproduce vegetatively.[10] The dependence of *R. microsporus* sporulation on *M. rhizoxinica* ensures that the symbiosis persists over time because the endosymbionts are translocated into the fungal spores during host reproduction.

Multiple investigations have shed light on various factors that are integral to the establishment and maintenance of the *R. microsporus-M. rhizoxinica* symbiosis. For example, *M. rhizoxinica* can invade *R. microsporus* by secreting chitinases via the type II secretion system (T2SS).[11] Bacterial invasion is further promoted by a bacterial linear lipopeptide (holrhizin) that reduces surface tension and biofilm formation.[12] In order

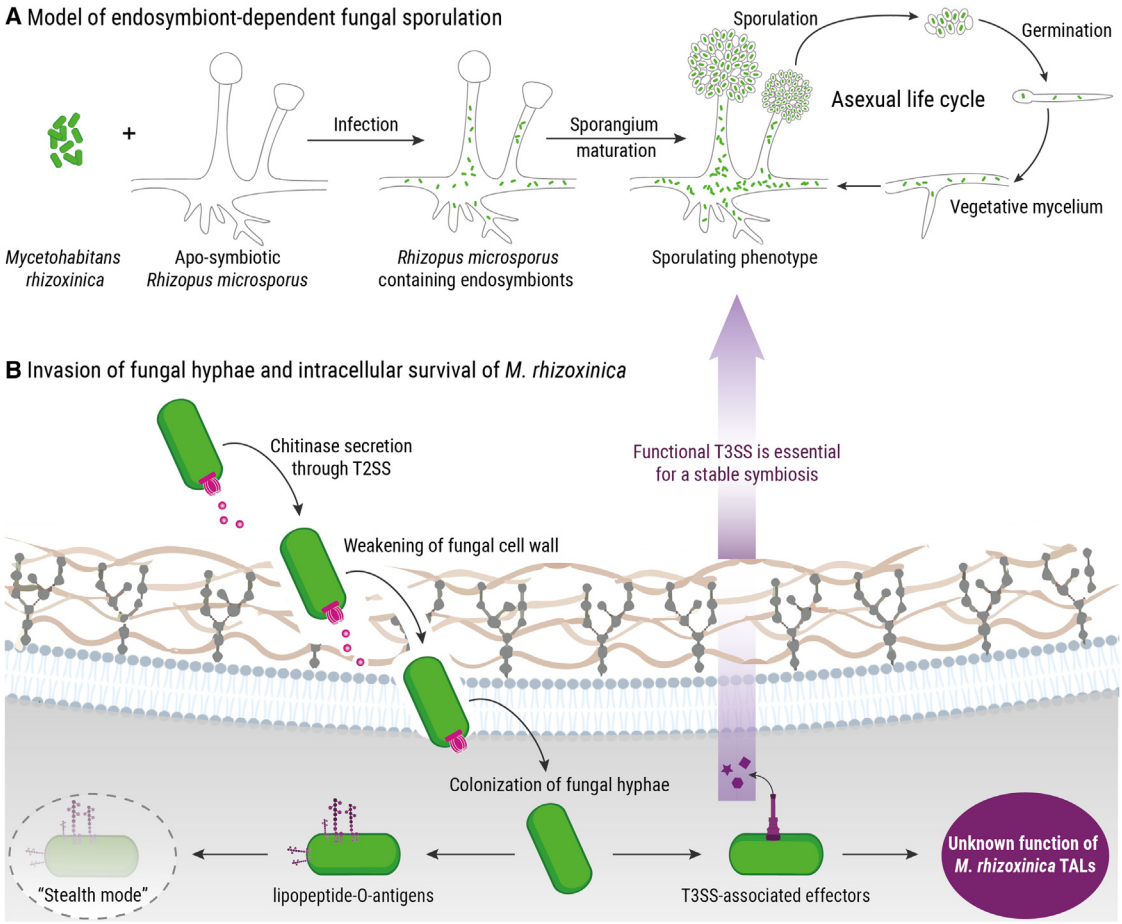

Figure 1. Schematic representation of endofungal bacteria and their intracellular lifestyle

(A) The Gram-negative bacterium *Mycetohabitans rhizoxinica* infects its fungal host *Rhizopus microsporus*, forming an endosymbiotic relationship. Fungal reproduction through spores is dependent on the presence of endosymbionts. Mature sporangia are absent in apo-symbiotic (endosymbiont-free) fungi.

(B) Entrance of *M. rhizoxinica* into the fungal hyphae is mediated by the secretion of effectors via a type 2 secretion system (T2SS). Once inside, *M. rhizoxinica* lives in "stealth mode" with the help of a specialized bacterial lipopeptide O-antigen. Although a functional type 3 secretion system (T3SS) is required for the formation of a stable symbiosis, the molecular function of the T3SS-secreted transcription activator-like (TAL) effectors in *M. rhizoxinica* is currently unknown.

to accommodate the endobacteria, the fungal host responds with upregulation of genes involved in cytoskeletal rearrangements, chitin synthesis, lipid metabolism, and quenching of reactive oxygen species.[13,14] Among the factors employed by *M. rhizoxinica* to persist within the fungal host is a specialized bacterial lipopeptide called O-antigen, which enables the endobacterium to live in "stealth mode."[15] In addition, a bacterial depsipeptide (habitasporin) and a functional type III secretion system (T3SS) are required for the formation of a stable symbiosis (Figure 1B).[16,17]

Upon initial physical contact with *R. microsporus*, nearly 60 T3SS-associated effector genes are upregulated in *M. rhizoxinica*.[13] Among them, perhaps the most well known are homologs of transcription activator-like (TAL) effectors from plant-pathogenic *Xanthomonas* and *Ralstonia* species.[18,19] TAL effectors localize to nuclei of plant hosts, where they bind to specific DNA sequences and act to induce expression of genes that aid bacterial colonization and virulence.[20] Although a *Mycetohabitans* TAL (MTAL) produced by *Mycetohabitans* sp. B13 is thought to increase the tolerance of *R. microsporus* to cell membrane stress,[21] there is relatively little known regarding the possible functions of MTALs in the interaction between *M. rhizoxinica* and its fungal host. Here, we show that *M. rhizoxinica* MTAL1 plays a key role in controlling the intracellular lifestyle of the endobacteria. Furthermore, we present the first real-time view of septa biogenesis in a Mucoromycota fungus, which leads to hyphal trapping of endobacteria incapable of secreting MTAL1.

RESULTS

M. rhizoxinica Δ*mtal1* does not influence hyphal morphology of *R. microsporus*

To investigate whether MTAL proteins are important for intracellular survival of *Mycetohabitans*, we performed a targeted gene deletion using a double-crossover strategy (Figures S1A and S1B).[16] We chose to focus on the most abundant *mtal* gene in *Mycetohabitans* spp., i.e., *mtal1*, and deleted this gene in *M. rhizoxinica* HKI-0454 to generate *M. rhizoxinica* Δ*mtal1* (*M. rhizoxinica* knockout, Figure S1C). *M. rhizoxinica* Δ*mtal1*

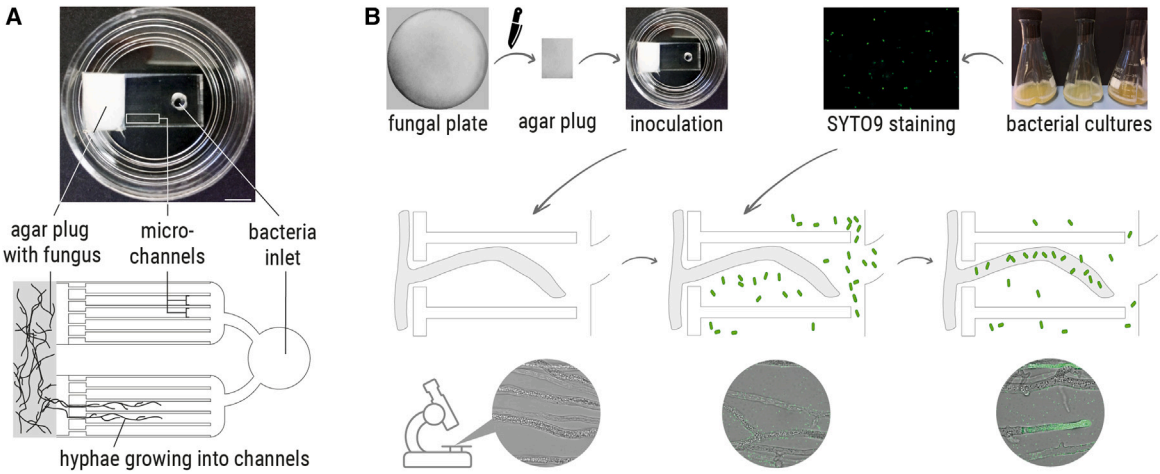

C Types of *R. microsporus* hyphae containing *M. rhizoxinica* Δ*mtal1*

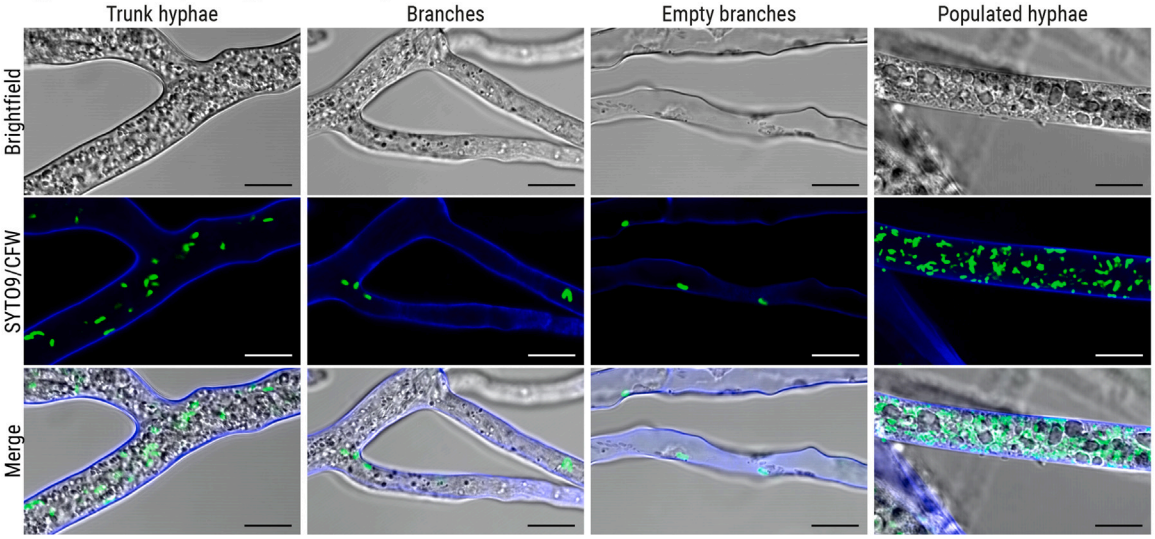

D

		Trunk hyphae	Branches	Empty branches	Populated hyphae
M1WT	0 hpi	47%	41%	12%	0%
	24 hpi	33%	36%	14%	17%
	48 hpi	44%	30%	16%	9%
Δ*mtal1*	0 hpi	48%	43%	9%	1%
	24 hpi	37%	33%	26%	4%
	48 hpi	38%	19%	32%	11%
Δ*mtal1* pBBRØ	0 hpi	47%	33%	17%	3%
	24 hpi	43%	21%	20%	17%
	48 hpi	32%	23%	27%	18%
Δ*mtal1* pBBR-*mtal1*	0 hpi	48%	20%	24%	5%
	24 hpi	46%	13%	26%	8%
	48 hpi	43%	17%	43%	7%

(legend on next page)

was transformed with pBBR_P$_{s12}$_*mtal1* (Figure S1D), an expression vector in which *mtal1* is under the control of a constitutive promoter, yielding the complemented strain *M. rhizoxinica* Δ*mtal1* pBBR-*mtal1* (complemented knockout). *M. rhizoxinica* Δ*mtal1* was transformed with pBBR_P$_{s12}$ to generate *M. rhizoxinica* Δ*mtal1* pBBRØ (empty vector control), a control strain containing the relevant empty vector.

In order to explore specific interactions between intracellular *M. rhizoxinica* Δ*mtal1* and fungal hyphae at the cellular level, we utilized a tailor-made microfluidic platform. This bacterial-fungal interaction (BFI) device enables fungal hyphae to be cultured in microchannels, thus allowing imaging of single hyphae over time (Figure 2A).[22] First, apo-symbiotic *R. microsporus* was grown in BFI devices filled with potato dextrose broth (PDB, Figure 2B). After 2 days of incubation, axenic *M. rhizoxinica* wild type, *M. rhizoxinica* Δ*mtal1*, *M. rhizoxinica* Δ*mtal1* pBBR∅, or *M. rhizoxinica* Δ*mtal1* pBBR-*mtal1* were stained with SYTO9 and then added individually to the bacteria inlet for co-incubation with apo-symbiotic *R. microsporus*. T3SS-deficient *M. rhizoxinica* (*M. rhizoxinica* Δ*sctC* or *M. rhizoxinica* Δ*sctT*)[16] and rhizoxin-deficient *M. rhizoxinica* (*M. rhizoxinica* Δ*rhiG*)[9] were also assessed in the assay. Both T3SS-deficient strains were previously reported to have limited ability to reinfect the fungus,[16] while deletion of *rhiG* causes disruption in the biosynthesis of the toxic macrolide rhizoxin, which should not impact the reinfection process.

Using light microscopy, we obtained high-resolution images of individual hyphae growing in the microchannels of the BFI devices. We observed four different types of hyphae, which were broadly classified as follows: (1) trunk hyphae, (2) branches, (3) empty branches, and (4) populated hyphae (Figures 2C, S2, and S3A). Trunk hyphae represent the main vegetative hyphae, which are characterized by their relatively large diameter (approximately 10–15 μm). They appear to be tightly packed with organelles (e.g., nuclei, vacuoles, mitochondria, etc.), which are transported through the hyphae at relatively high speed (Video S1). This hyphal classification has been described for members of the Basidiomycetes and Ascomycetes, but rarely for Mucoromycota.[23,24] We also observed smaller side hyphae, which are either filled with cellular components (branches) or are empty (empty branches). Populated hyphae represent another type of side hyphae, which are filled with organelles and are similar in diameter to the trunk hyphae. In addition, they show strong green fluorescence, which is indicative of high bacterial cell numbers (Figure 2C). Comparison of the mycelium area revealed a similar distribution of individual types of hyphae over time and regardless of the infecting *M. rhizoxinica* strain (Figures 2D and S3B; Data S1).

High bacterial load of *M. rhizoxinica* Δ*mtal1* in fungal hyphae

Intrigued by the apparent high cell number of *M. rhizoxinica* in populated hyphae, we quantified the number of endohyphal bacteria after colonization of *R. microsporus* by SYTO9-stained *M. rhizoxinica* in BFI devices. The bacterial load inside the fungal hyphae was measured by calculating the number of fluorescent endohyphal bacteria from the integrated density at 485/498 nm (Figure 3A). In comparison with when apo-symbiotic *R. microsporus* is colonized by *M. rhizoxinica* wild type, both *M. rhizoxinica* Δ*mtal1* and *M. rhizoxinica* Δ*mtal1* pBBR∅ show significantly higher cell numbers ($p < 0.05$) after 1 day (Data S2A–S2D). In contrast, the bacterial load of hyphae colonized by *M. rhizoxinica* Δ*mtal1* pBBR-*mtal1* is similar to that of *M. rhizoxinica* wild type (Figure 3A; Data S2A–S2D). As expected, endobacteria were absent from hyphae when the T3SS-deficient *M. rhizoxinica* strains were co-cultured with the apo-symbiotic fungus (Figures S3C–S3E). In contrast, rhizoxin-deficient bacteria are present in fungal hyphae at a similar level to the wild type (Figures S3C–S3E; Data S2E–S2H).

The counts of endofungal *M. rhizoxinica* wild type, *M. rhizoxinica* Δ*mtal1*, *M. rhizoxinica* Δ*mtal1* pBBR∅, and *M. rhizoxinica* Δ*mtal1* pBBR-*mtal1* at the 24 h time point are not significantly different from those at 48 h (Figure 3A; Data S2A–S2D), suggesting that fungal reinfection takes place within 24 h of their introduction. However, it is important to consider that a potential increase in bacterial cell numbers after 24 h may not have been detected due to dilution of the staining intensity caused by bacterial proliferation and bleaching of SYTO9.[25] To minimize SYTO9-bleaching, light exposure was kept to a minimum by using a short exposure time (100 ms). In addition, axenic SYTO9-stained *M. rhizoxinica* wild type, *M. rhizoxinica* Δ*mtal1*, *M. rhizoxinica* Δ*mtal1* pBBR∅, and *M. rhizoxinica* Δ*mtal1* pBBR-*mtal1* were shown to remain detectably stained after culturing for 24 and 48 h in refreshed medium (Figure S4).

When the bacterial load was quantified for each individual type of hyphae, we noticed that the cell number of *M. rhizoxinica* Δ*mtal1* in populated hyphae is significantly higher ($p < 0.0002$) after 2 days of co-incubation than after 1 day (Figure 3B; Data S3A–S3D). Populated hyphae also contain a higher number of *M. rhizoxinica* Δ*mtal1* pBBR∅ after 48 h, reaching a similar cell number as *M. rhizoxinica* Δ*mtal1*. Genetic complementation

Figure 2. Phenotypic observations of *R. microsporus* co-cultivated with *M. rhizoxinica* wild type or *M. rhizoxinica* Δ*mtal1* in bacterial-fungal interaction (BFI) devices

(A) Photograph and simplified illustration showing the BFI device in a glass Petri dish. The BFI device is made of a patterned poly(dimethylsiloxane) layer bonded to a glass-bottomed dish to form microchannels, which were filled with PDB. Scale bars: 5 mm. Two-dimensional representation showing the narrow entry points into the microchannels that limit the number of hyphae that can enter the device.

(B) Illustration showing the workflow. An agar plug containing apo-symbiotic *R. microsporus* is placed in direct contact with the microchannels. After 2 days of incubation, hyphae are growing inside the microchannels, and SYTO9-stained bacterial strains are introduced into the microchannels via the "bacteria inlet." Fungal reinfection is monitored over 48 h, and microscopic images are taken every 24 h.

(C) Microscopic images of *R. microsporus* (stained with calcofluor white [CFW]) co-cultivated with *M. rhizoxinica* Δ*mtal1* (SYTO9-stained) depicting four types of hyphae. Scale bars: 10 μm.

(D) The fungal mycelium area (as a percentage) of each type of hyphae was measured over a 48-h time period of co-incubation in BFI devices. At time point 0, cultures of *M. rhizoxinica* wild type (M1WT), *M. rhizoxinica* Δ*mtal1*, *M. rhizoxinica* Δ*mtal1* pBBR∅, or *M. rhizoxinica* Δ*mtal1* pBBR-*mtal1* were stained with SYTO9, individually added to the inlet, and co-incubated with apo-symbiotic *R. microsporus*. Images were taken at the time of infection (0 h post infection [hpi]), as well as 24 and 48 hpi. n = 3 biological replicates ± SEM (Data S1A–S1D). See also Figures S2, S3A, and S3B.

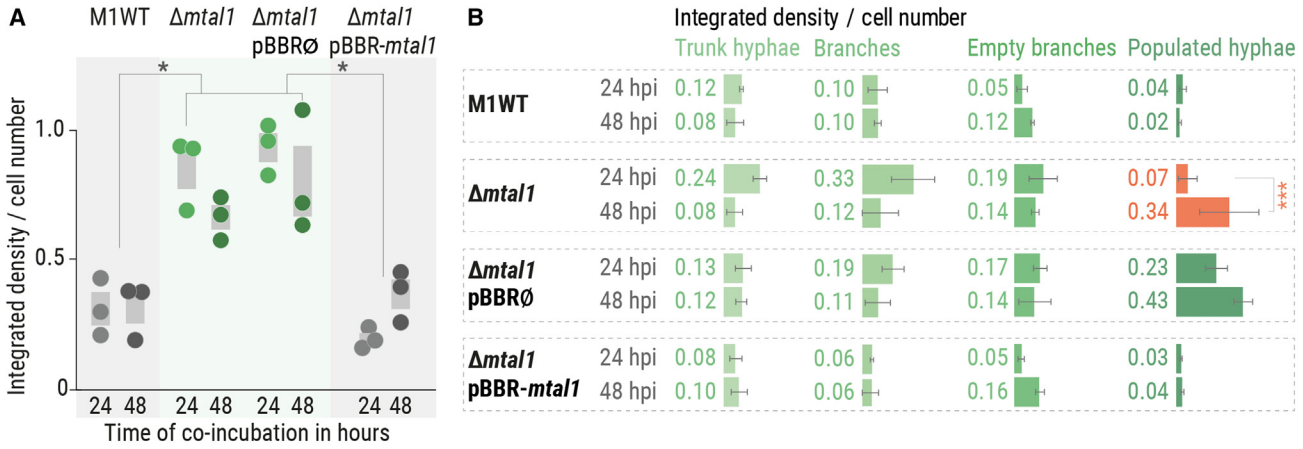

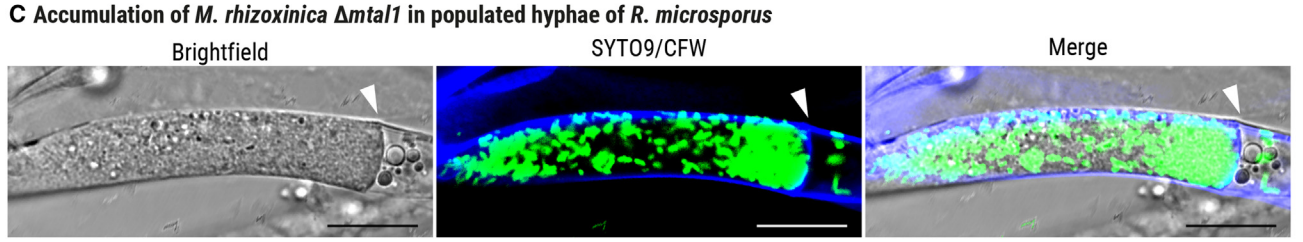

Figure 3. Quantification of MTAL1-deficient *M. rhizoxinica* inside *R. microsporus*

(A) Apo-symbiotic *R. microsporus* was individually co-incubated with SYTO9-stained *M. rhizoxinica* wild type (M1WT), *M. rhizoxinica* Δ*mtal1*, *M. rhizoxinica* Δ*mtal1* pBBR∅, or *M. rhizoxinica* Δ*mtal1* pBBR-*mtal1* for 48 h. After fluorescence microscopy at 485/498 nm, the integrated density per bacterial cell number was calculated for both time points (24 and 48 hpi). Dots represent three independent replicates (n = 3 biological replicates) ± SEM (gray bars). One-way ANOVA with Tukey's multiple comparison test (*$p < 0.05$, Data S2A–S2D).

(B) The integrated density per cell number was measured for each individual type of hyphae. n = 3 biological replicates ± SEM. One-way ANOVA with Tukey's multiple comparison test (***$p < 0.0002$, Data S3A–S3D).

(C) Fluorescence microscopy images showing the accumulation of *M. rhizoxinica* Δ*mtal1* (green) in populated hyphae of *R. microsporus* (blue). Septa are indicated by an arrow head. Scale bars: 10 μm. See also Figures S3C–S3E and S4.

restores wild-type behavior, with *M. rhizoxinica* Δ*mtal1* pBBR-*mtal1* distribution across the different types of hyphae being similar to that of *M. rhizoxinica* wild type (Figure 3B; Data S3A–S3D). Accumulation of *M. rhizoxinica* Δ*mtal1* and *M. rhizoxinica* Δ*mtal1* pBBR∅ in populated hyphae is clearly visible in microscopic images (Figures 3C and S2B). In contrast, accumulation of *M. rhizoxinica* wild type, *M. rhizoxinica* Δ*mtal1* pBBR-*mtal1*, and *M. rhizoxinica* Δ*rhiG* in populated hyphae was only occasionally observed. As expected, populated hyphae are absent in *R. microsporus* co-cultivated with T3SS-deficient *M. rhizoxinica* because these strains are unable to effectively colonize fungal hyphae (Figure S3D; Data S3E–S3H). Taken together, these results reveal that MTAL1-deficient *M. rhizoxinica* reaches higher cell densities than *M. rhizoxinica* wild type in *R. microsporus*-populated hyphae.

M. rhizoxinica Δ*mtal1* colonization of *R. microsporus* causes hyphal septation

To visualize the process by which *M. rhizoxinica* Δ*mtal1* reaches high cell densities in fungal hyphae, the colonization of *R. microsporus* by *M. rhizoxinica* Δ*mtal1* was monitored in real time using a BFI device (Figure 4A; Video S1). First, *M. rhizoxinica* Δ*mtal1* penetrates and enters selected hyphae of *R. microsporus*. Following colonization, the bacterial cells accumulate in high numbers (strong green fluorescent signal), and a septum is formed at the base of these hyphae in a relatively short amount of time (approximately 3 min). As a result, the cytoplasmic flow between colonized hyphae and the remaining fungal mycelium is abolished, leading to the physical containment of bacteria (Video S1).

Intrigued by our observation of septa formation in *R. microsporus*, we analyzed the number of septa formed after fungal reinfection by *M. rhizoxinica* strains in a BFI device. The data were normalized by dividing the septa number by the mycelium area (in μm) that was analyzed (Figure 4B). Although septa formation occurs occasionally in hyphae containing *M. rhizoxinica* wild type, we observed a significant increase in septa formation in hyphae containing *M. rhizoxinica* Δ*mtal1* and *M. rhizoxinica* Δ*mtal1* pBBR∅ after 24 h of co-incubation ($p < 0.05$, Figure 4B; Data S4A–S4D). This increase in septa formation is maintained at the 48 h time point. In contrast, the number of septa in hyphae colonized by *M. rhizoxinica* Δ*mtal1* pBBR-*mtal1*, T3SS-deficient *M. rhizoxinica* strains (*M. rhizoxinica* Δ*sctC* and *M. rhizoxinica* Δ*sctT*), and *M. rhizoxinica* Δ*rhiG* is comparable to the wild type (Figures 4B, S5A, and S5B; Data S4E–S4H).

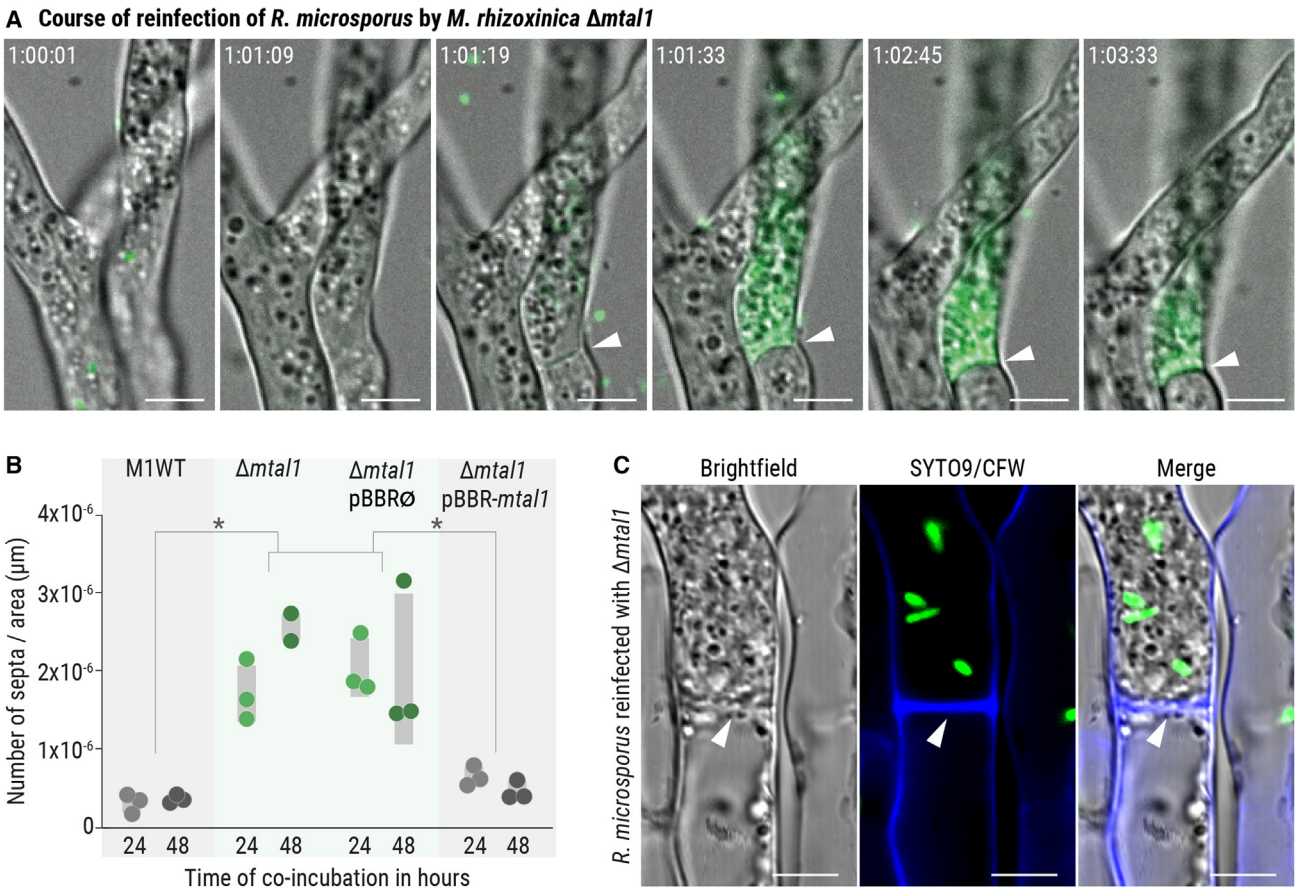

Figure 4. Formation of septa after colonization of *R. microsporus* by MTAL1-deficient *M. rhizoxinica*

(A) Course of colonization of *R. microsporus* by *M. rhizoxinica* Δ*mtal1*. Colonization was monitored over time using fluorescence microscopy (Video S1). Arrowheads indicate the formation of septa. Scale bars: 5 μm.

(B) The number of septa per hyphal area (in μm) was calculated for *M. rhizoxinica* wild type (M1WT), *M. rhizoxinica* Δ*mtal1*, *M. rhizoxinica* Δ*mtal1* pBBR∅, and *M. rhizoxinica* Δ*mtal1* pBBR-*mtal1*. Dots represent three independent replicates (n = 3 biological replicates) ± SEM (gray bars). One-way ANOVA with Tukey's multiple comparison test (*$p < 0.05$, Data S4A–S4D).

(C) Fluorescence microscopy images showing the formation of septa (indicated by an arrow head) in *R. microsporus* (blue stain) colonized by *M. rhizoxinica* Δ*mtal1* (green). Scale bars: 5 μm. See also Figures S5A and S5B.

To confirm that the observed septa are true septa, fungal mycelium containing SYTO9-stained *M. rhizoxinica* wild type, *M. rhizoxinica* Δ*mtal1*, *M. rhizoxinica* Δ*mtal1* pBBR∅, or *M. rhizoxinica* Δ*mtal1* pBBR-*mtal1* was counter-stained with calcofluor white, a fungal cell-wall-specific dye. Fluorescence microscopy images reveal that septa are indeed composed of fungal cell wall material (Figures 4C and S5B). This formation of septa may represent a mechanism to limit hyphal damage caused by MTAL1-deficient *M. rhizoxinica*, considering that *R. microsporus* is known to produce septa to wall off old or injured hyphae.[23,26]

Survival of trapped *M. rhizoxinica* Δ*mtal1* is reduced in *R. microsporus*-populated hyphae

Based on the observation that septa formation stops the cytoplasmic flow between populated hyphae and the remaining fungal mycelium, we investigated whether trapped bacteria are alive in these hyphae. Using a bacterial LIVE/DEAD stain (SYTO9/propidium iodide [PI]) we observed that the majority of bacteria in trunk hyphae, branches, and empty branches are alive independent of MTAL1 production because *M. rhizoxinica* Δ*mtal1* and *M. rhizoxinica* Δ*mtal1* pBBR∅ have ratios of live vs. dead that are similar to those of *M. rhizoxinica* wild type and *M. rhizoxinica* Δ*mtal1* pBBR-*mtal1* (Figure 5A; Data S5). In contrast, the survival of *M. rhizoxinica* Δ*mtal1* and *M. rhizoxinica* Δ*mtal1* pBBR∅ in populated hyphae is significantly reduced compared with *M. rhizoxinica* wild type and *M. rhizoxinica* Δ*mtal1* pBBR-*mtal1* ($p < 0.002$, Figure 5A; Data S5). These results were confirmed by microscopic images showing mainly dead (red stained) *M. rhizoxinica* Δ*mtal1* and *M. rhizoxinica* Δ*mtal1* pBBR∅ in populated hyphae, while the majority of *M. rhizoxinica* wild type and *M. rhizoxinica* Δ*mtal1* pBBR-*mtal1* are alive (green stained) in these hyphae (Figure 5B). These results suggest decreased *M. rhizoxinica* survival in the absence of MTAL1 (Figure 6).

It should be considered that LIVE/DEAD staining using SYTO9 and PI may underestimate bacterial viability. SYTO9 (live stain) can stain live cells with different efficiencies,[25] while PI (dead

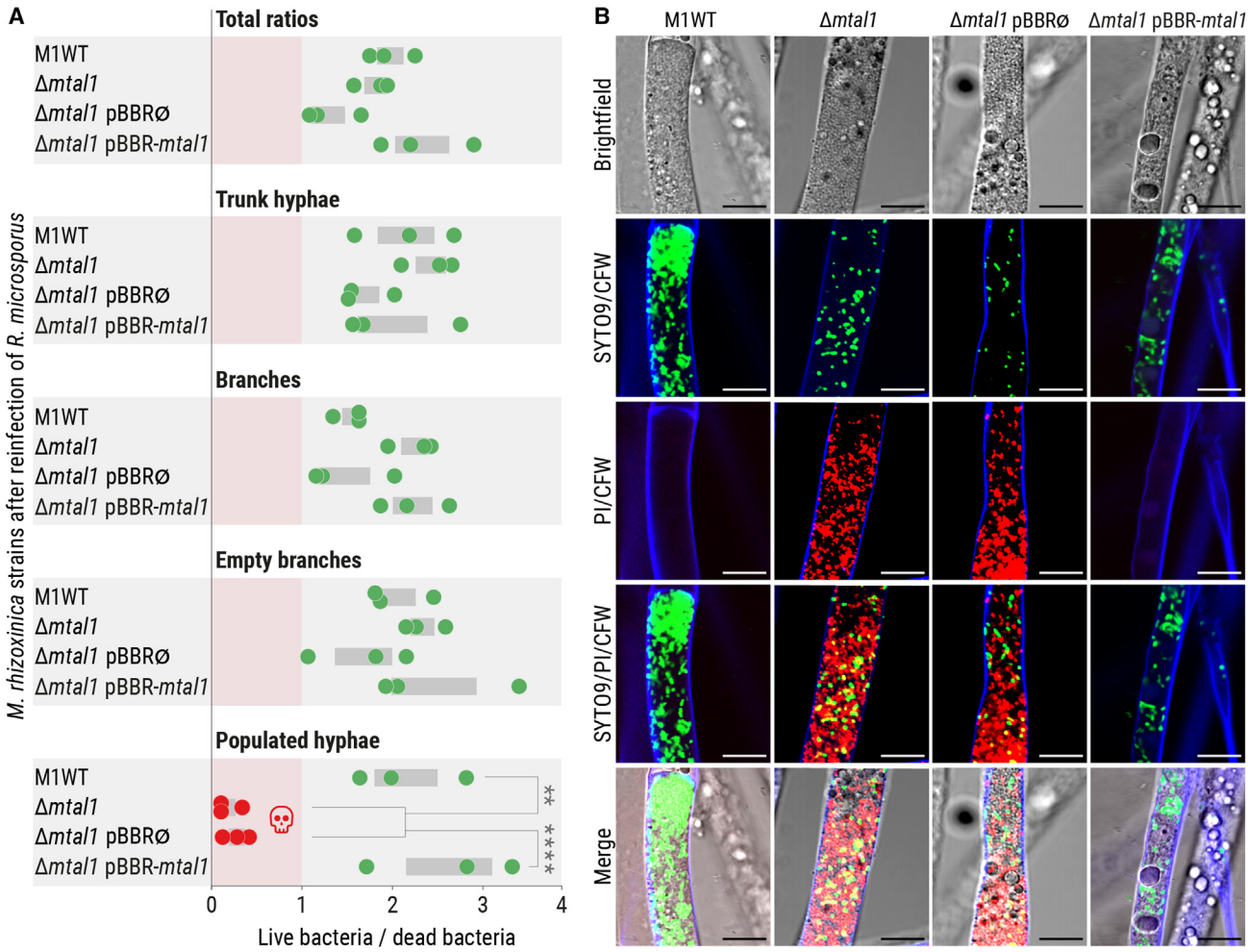

Figure 5. Viability test of *M. rhizoxinica* following colonization of *R. microsporus*

(A) Viability of *M. rhizoxinica* wild type (M1WT), *M. rhizoxinica* Δ*mtal1*, *M. rhizoxinica* Δ*mtal1* pBBR∅, and *M. rhizoxinica* Δ*mtal1* pBBR-*mtal1* inside *R. microsporus* after 72 h of co-cultivation in a bacterial-fungal interaction (BFI) device. Co-cultures were stained with LIVE/DEAD BacLight fluorescent dyes inside the BFI device. Following fluorescence microscopy, the integrated density was calculated for both live (SYTO9-stained) and dead bacteria (propidium iodide-stained [PI]) using Fiji. The ratio (live/dead) was plotted for the total number of bacteria and for each individual type of hyphae. Dots represent three independent replicates (n = 3 biological replicates) ± SEM (gray bars). One-way ANOVA with Tukey's multiple comparison test (**$p < 0.002$, ****$p < 0.0001$, Data S5).

(B) Microscopic images of *R. microsporus* colonized by *M. rhizoxinica* wild type (M1WT), *M. rhizoxinica* Δ*mtal1*, *M. rhizoxinica* Δ*mtal1* pBBR∅, or *M. rhizoxinica* Δ*mtal1* pBBR-*mtal1* stained with LIVE/DEAD BacLight fluorescent dyes. Scale bars: 10 μm. See also Figure S5C.

stain) has a strong binding affinity to extracellular nucleic acids, a major component of bacterial biofilms.[27] Because *M. rhizoxinica* is a known biofilm producer,[28] we performed LIVE/DEAD stains of axenic cultures before co-incubation in BFI devices. The majority of the cells stained green with negligible red staining (Figure S5C), indicating that underestimation of bacterial viability due to PI binding to extracellular nucleic acids is unlikely.

DISCUSSION

Both pathogenic and symbiotic bacteria can invade and control their eukaryotic hosts by employing effector molecules.[29,30] One prominent example is the TAL effectors, a family of highly homologous proteins secreted by the T3SS that have been implicated in the virulence of numerous plant pathogens.[31–33] In recent years, TALs have become popular as biotechnological tools due to their ability to manipulate DNA in a site-directed manner.[34] Consequently, TAL homologs have been identified in a wide range of bacterial species, including *M. rhizoxinica* (MTAL1, MTAL2, and MTAL3).[35] In this study, we combined genetic and phenotypic studies to functionally characterize MTAL1 of the fungal endosymbiont *M. rhizoxinica*. Targeted gene knockouts resulted in MTAL1-deficient bacteria that became trapped in side hyphae through the formation of septa, signifying that MTAL1 is an important symbiosis factor for the *Rhizopus-Mycetohabitans* interaction.

By means of a tailor-made microfluidic device,[22] we show that the *R. microsporus* mycelium is composed of four phenotypically distinct types of hyphae (trunk hyphae, branches, empty branches, and populated hyphae). These fungal hyphae types have been rarely observed among the Mucoromycota,[23] and this is the first time that different cell types have been described

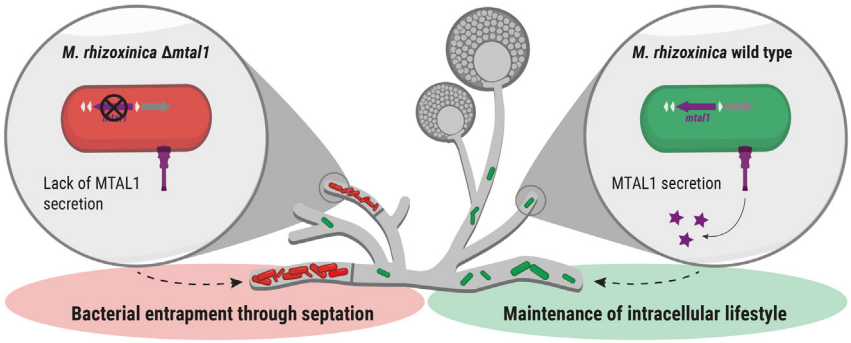

Figure 6. Schematic model of the intracellular survival of endofungal bacteria

The endosymbiotic bacterium *Mycetohabitans rhizoxinica* secretes transcription activator-like effector 1 (MTAL1) via the type 3 secretion system, which is essential for its survival within *R. microsporus* (green). Absence of MTAL1 leads to entrapment of *M. rhizoxinica* through fungal septation and subsequent bacterial cell death (red).

for *R. microsporus*. The vegetative main hyphae, or so-called trunk hyphae,[36,37] are important for transporting intracellular material across the mycelium at relatively high speeds. This allows *R. microsporus* and fungi in general to cope well with heterogeneous distributions of soil nutrients in their natural habitat.[24] In addition, cytoplasmic flow enables the free migration of *M. rhizoxinica* throughout the host mycelium.[38] Hyphae serving as dispersal vectors for motile bacteria are an important feature of BFI ecology[39] and are thought to promote colonization of new ecological niches.[40]

Fluorescence microscopy combined with microfluidics was used to gain a deeper understanding of the interaction between MTAL1-deficient *M. rhizoxinica* and *R. microsporus*. We have demonstrated (1) efficient fungal reinfection by MTAL1 knockout strains within 1 day and (2) accumulation and trapping of these strains in side hyphae after 2 days. These infected side hyphae (populated hyphae) are then walled off from the remaining mycelium via the formation of septa, which abrogates cytosolic exchange. In this way, *M. rhizoxinica*, which normally moves freely within the mycelium,[10] becomes physically restricted (Figure 6). The observed increase in bacterial density may be caused by the ongoing cell division of MTAL1-deficient *M. rhizoxinica* while trapped. Alternatively, it is plausible that MTAL1-deficient bacteria are redistributed inside the fungal mycelium after reinfection and subsequently accumulate in side hyphae, as total bacterial numbers reach a maximum after 1 day and a significant increase within populated hyphae is observed after 2 days. We propose that the spatial separation of MTAL1-deficient symbionts in walled-off hyphae may allow the fungal host to impede interactions with non-beneficial symbionts.[41] Although such compartmentalization in fungi is only described for arbuscular mycorrhizal fungi, its benefits to the host are well documented in a wide range of host-microbe mutualisms (e.g., insects and bacteria, legumes and rhizobia, and squid and *Vibrio*).[41] For example, mycorrhiza form partial compartments in the host plant's root tissue (arbuscules). The host uses these compartments to monitor the quality of the symbiont and subsequently regulate symbiont success.[42] A similar regulatory mechanism could be used by *R. microsporus* to protect itself against colonization by MTAL1-deficient bacteria. Because the majority of trapped MTAL1-deficient bacteria are dead, it could be that bacterial cell death results from a host-produced toxic factor. Alternatively, entrapment may result in an insufficiency of the host-derived metabolites and lipids on which *M. rhizoxinica* depends.[14,43]

Our visualization of septa formation by *R. microsporus* is one of the most surprising results because vegetative hyphae of Mucoromycota generally lack regular septa.[23] Interestingly, *R. microsporus* has been observed to produce septa as separators between mycelia and spore-forming structures.[23,26] Thus, given that *R. microsporus* grown submerged in liquid medium struggles to produce mature sporangia, it could be that populated hyphae represent abortive sporangia due to the set-up of the microfluidics devices. However, considering that the persistence of the symbiosis is dependent on spores containing healthy endobacteria,[10] we would expect the majority of the trapped MTAL1-deficient endobacteria to be alive (as seen in the rare instances of trapped wild-type bacteria). Since the majority of MTAL1-deficient bacteria are dead, we reason that it is unlikely that populated hyphae represent abortive sporangia. Instead, it is possible that septa are formed as a response to limit hyphal damage caused by MTAL1-deficient bacteria because Mucoromycota fungi can form septa to wall off old or injured hyphae.[23,26] In addition, induced host suicide by bacteria is a mechanism that is well described in plant-pathogen interactions. For example, TALs from *X. campestris* induce a suicide gene in resistant plants, causing programmed cell death in the host and thereby preventing the pathogen from spreading.[44] Another mechanism to restrict the horizontal propagation of harmful cytoplasmic components in filamentous fungi is vegetative (heterokaryon) incompatibility.[45] In *Neurospora crassa*, hyphal fusion of two heterokaryon-incompatible individuals leads to septa formation and subsequent death of the resulting compartments.[46] This behavior appears strikingly similar to the formation of septa by *R. microsporus* after colonization by MTAL1-deficient *M. rhizoxinica*. Although it remains to be investigated whether populated hyphae are dead and/or damaged, it is nonetheless an interesting proposition that MTAL1-deficient endobacteria may trigger a response similar to nonself-recognition in Mucoromycota fungi.

Notably, the MTAL1 proteins described in this study are the first TAL-related proteins whose absence causes an increase in host colonization. In contrast, TAL proteins of plant pathogens induce susceptibility genes, which leads to a dramatic increase in bacterial cell numbers in the host.[47] Thus, MTAL1 might represent DNA-binding proteins with a function different from TALs[34] because multiple unrelated DNA-binding proteins are known to aid host colonization by various pathogens and symbionts.[29] It is conceivable that *R. microsporus* perceives *M. rhizoxinica* lacking MTAL1 not as an endosymbiont but as a pathogen. Indeed, *M. rhizoxinica* likely was initially a parasite before becoming a mutualist,[14,48,49] with *R. microsporus* having acquired

resistance against the potent phytotoxin (rhizoxin) produced by *M. rhizoxinica*.[49] Thus, MTAL1 proteins might represent an important factor for the maintenance of the mutualistic relationship in this BFI,[21] and their absence may cause a reversion from a mutualistic to a parasitic lifestyle. Our data designating MTAL1 as a symbiosis factor in the *R. microsporus-M. rhizoxinica* relationship illuminate the ''sliding scale'' nature of BFIs, wherein symbionts can act as mutualists or pathogens depending on the genetic context.[50]

In summary, we show that MTAL1-deficient endosymbionts successfully recolonize the host but become trapped in side hyphae due to the formation of septa. These observations represent an unprecedented case in which bacterial colonization induces biogenesis of septa in a Mucoromycota fungus, a likely defense strategy of the host. Based on microscopic investigations, it appears that MTAL1-deficient mutants are perceived as pathogens in the fungal cytosol, in accordance with a plausible antagonism-mutualism shift in the evolution of this microbial symbiosis. Our results not only offer insight into the dynamic interactions between bacteria and fungi but also open new avenues of research into endobacterial control of fungal host physiology.

STAR★METHODS

Detailed methods are provided in the online version of this paper and include the following:

- KEY RESOURCES TABLE
- RESOURCE AVAILABILITY
  - Lead contact
  - Materials availability
  - Data and code availability
- EXPERIMENTAL MODEL AND SUBJECT DETAILS
- METHOD DETAILS
  - Generation of *M. rhizoxinica* Δ*mtal1* strains
  - Generation of genetically complemented *M. rhizoxinica* Δ*mtal1* strains
  - Inoculation of bacterial-fungal interaction devices with fungus
  - Bacterial inoculation into bacterial-fungal interaction devices
  - Live-cell imaging of bacterial-fungal interactions
  - Imaging of bacterial survival inside of bacterial-fungal interaction devices
  - Quantification of bacterial cells inside of fungal hyphae
  - Imaging of axenic bacterial cultures
  - Imaging of fungal septa
- QUANTIFICATION AND STATISTICAL ANALYSIS

SUPPLEMENTAL INFORMATION

Supplemental information can be found online at https://doi.org/10.1016/j.cub.2023.05.028.

ACKNOWLEDGMENTS

We thank S. Lindner for assistance with image analyses. I.R. is grateful for financial support from the European Union's Horizon 2020 Research and Innovation Program under the Marie Skłodowska-Curie grant agreement no. 794343. Financial support by the Deutsche Forschungsgemeinschaft (DFG, German Research Foundation) under Germany's Excellence Strategy—EXC 2051 (Cluster of Excellence ''Balance of the Microverse'') Project-ID 390713860 and the SFB 1127 ChemBioSys, Project-ID 239748522, and the Leibniz Award (to C.H.); the JSMC to Z.U.; and the Swiss National Science Foundation in the form of an Ambizione Career Grant (PZ00P2_168005) to C.E.S. is gratefully acknowledged. We thank the Microverse Imaging Center and Aurélie Jost for providing microscope facility support for data acquisition. The ELYRA 7 (used for producing images of axenic bacterial cultures) was funded by the Free State of Thuringia with grant number 2019 FGI 0003. The Microverse Imaging Center is funded by the DFG under Germany's Excellence Strategy—EXC 2051, Project-ID 390713860.

AUTHOR CONTRIBUTIONS

I.R. conceived the idea, developed the study design, interpreted the data, and wrote the manuscript. P.W. designed plasmids and generated complemented strains. Z.U. conceived the idea and generated the *mtal1* knockout strain. C.E.S. designed and manufactured microfluidic devices and revised the manuscript. J.K. assisted with plasmid design. E.M.M. assisted in data interpretation and manuscript revision. N.M. conceived the idea. I.F. assisted with method development of image analysis. F.H. assisted in data interpretation and manuscript revision. C.H. conceived the idea and drafted and revised the manuscript.

DECLARATION OF INTERESTS

The authors declare no competing interests.

Received: November 4, 2022
Revised: March 30, 2023
Accepted: May 12, 2023
Published: June 9, 2023

REFERENCES

1. Wernegreen, J.J. (2012). Endosymbiosis. Curr. Biol. *22*, R555–R561. https://doi.org/10.1016/j.cub.2012.06.010.
2. Sachs, J.L., Skophammer, R.G., and Regus, J.U. (2011). Evolutionary transitions in bacterial symbiosis. Proc. Natl. Acad. Sci. USA *108*, 10800–10807. https://doi.org/10.1073/pnas.1100304108.
3. Pawlowska, T.E., Gaspar, M.L., Lastovetsky, O.A., Mondo, S.J., Real-Ramirez, I., Shakya, E., and Bonfante, P. (2018). Biology of fungi and their bacterial endosymbionts. Annu. Rev. Phytopathol. *56*, 289–309. https://doi.org/10.1146/annurev-phyto-080417-045914.
4. Bonfante, P., and Desirò, A. (2017). Who lives in a fungus? The diversity, origins and functions of fungal endobacteria living in *Mucoromycota*. ISME J. *11*, 1727–1735. https://doi.org/10.1038/ismej.2017.21.
5. Partida-Martinez, L.P., and Hertweck, C. (2005). Pathogenic fungus harbours endosymbiotic bacteria for toxin production. Nature *437*, 884–888. https://doi.org/10.1038/nature03997.
6. Partida-Martinez, L.P., and Hertweck, C. (2007). A gene cluster encoding rhizoxin biosynthesis in *Burkholderia rhizoxina*, the bacterial endosymbiont of the fungus *Rhizopus microsporus*. ChemBioChem *8*, 41–45. https://doi.org/10.1002/cbic.200600393.
7. Estrada-de Los Santos, P., Palmer, M., Chávez-Ramírez, B., Beukes, C., Steenkamp, E.T., Briscoe, L., Khan, N., Maluk, M., Lafos, M., Humm, E., et al. (2018). Whole genome analyses suggests that Burkholderia sensu lato contains two additional novel genera (*Mycetohabitans* gen. nov., and *Trinickia* gen. nov.): implications for the evolution of diazotrophy and nodulation in the *Burkholderiaceae*. Genes *9*. https://doi.org/10.3390/genes9080389.
8. Lackner, G., and Hertweck, C. (2011). Impact of endofungal bacteria on infection biology, food safety, and drug development. PLoS Pathog. *7*, e1002096. https://doi.org/10.1371/journal.ppat.1002096.

9. Scherlach, K., Busch, B., Lackner, G., Paszkowski, U., and Hertweck, C. (2012). Symbiotic cooperation in the biosynthesis of a phytotoxin. Angew. Chem. Int. Ed. Engl. *51*, 9615–9618. https://doi.org/10.1002/anie.201204540.

10. Partida-Martinez, L.P., Monajembashi, S., Greulich, K.O., and Hertweck, C. (2007). Endosymbiont-dependent host reproduction maintains bacterial-fungal mutualism. Curr. Biol. *17*, 773–777. https://doi.org/10.1016/j.cub.2007.03.039.

11. Moebius, N., Üzüm, Z., Dijksterhuis, J., Lackner, G., and Hertweck, C. (2014). Active invasion of bacteria into living fungal cells. eLife *3*, e03007. https://doi.org/10.7554/eLife.03007.

12. Niehs, S.P., Scherlach, K., and Hertweck, C. (2018). Genomics-driven discovery of a linear lipopeptide promoting host colonization by endofungal bacteria. Org. Biomol. Chem. *16*, 8345–8352. https://doi.org/10.1039/c8ob01515e.

13. Lastovetsky, O.A., Krasnovsky, L.D., Qin, X., Gaspar, M.L., Gryganskyi, A.P., Huntemann, M., Clum, A., Pillay, M., Palaniappan, K., Varghese, N., et al. (2020). Molecular dialogues between early divergent fungi and bacteria in an antagonism versus a mutualism. mBio *11*, e02088-20. https://doi.org/10.1128/mBio.02088-20.

14. Lastovetsky, O.A., Gaspar, M.L., Mondo, S.J., LaButti, K.M., Sandor, L., Grigoriev, I.V., Henry, S.A., and Pawlowska, T.E. (2016). Lipid metabolic changes in an early divergent fungus govern the establishment of a mutualistic symbiosis with endobacteria. Proc. Natl. Acad. Sci. USA *113*, 15102–15107. https://doi.org/10.1073/pnas.1615148113.

15. Leone, M.R., Lackner, G., Silipo, A., Lanzetta, R., Molinaro, A., and Hertweck, C. (2010). An unusual galactofuranose lipopolysaccharide that ensures the intracellular survival of toxin-producing bacteria in their fungal host. Angew. Chem. Int. Ed. Engl. *49*, 7476–7480. https://doi.org/10.1002/anie.201003301.

16. Lackner, G., Moebius, N., and Hertweck, C. (2011). Endofungal bacterium controls its host by an hrp type III secretion system. ISME J. *5*, 252–261. https://doi.org/10.1038/ismej.2010.126.

17. Niehs, S.P., Scherlach, K., Dose, B., Uzum, Z., Stinear, T.P., Pidot, S.J., and Hertweck, C. (2022). A highly conserved gene locus in endofungal bacteria codes for the biosynthesis of symbiosis-specific cyclopeptides. Proc. Natl. Acad. Sci. USA *1*, pgac152. https://doi.org/10.1093/pnasnexus/pgac152.

18. Juillerat, A., Bertonati, C., Dubois, G., Guyot, V., Thomas, S., Valton, J., Beurdeley, M., Silva, G.H., Daboussi, F., and Duchateau, P. (2014). BurrH: a new modular DNA binding protein for genome engineering. Sci. Rep. *4*, 3831. https://doi.org/10.1038/srep03831.

19. de Lange, O., Wolf, C., Dietze, J., Elsaesser, J., Morbitzer, R., and Lahaye, T. (2014). Programmable DNA-binding proteins from *Burkholderia* provide a fresh perspective on the TALE-like repeat domain. Nucleic Acids Res. *42*, 7436–7449. https://doi.org/10.1093/nar/gku329.

20. Scholze, H., and Boch, J. (2011). TAL effectors are remote controls for gene activation. Curr. Opin. Microbiol. *14*, 47–53. https://doi.org/10.1016/j.mib.2010.12.001.

21. Carter, M.E., Carpenter, S.C.D., Dubrow, Z.E., Sabol, M.R., Rinaldi, F.C., Lastovetsky, O.A., Mondo, S.J., Pawlowska, T.E., and Bogdanove, A.J. (2020). A TAL effector-like protein of an endofungal bacterium increases the stress tolerance and alters the transcriptome of the host. Proc. Natl. Acad. Sci. USA *117*, 17122–17129. https://doi.org/10.1073/pnas.2003857117.

22. Stanley, C.E., Stöckli, M., van Swaay, D., Sabotič, J., Kallio, P.T., Künzler, M., deMello, A.J., and Aebi, M. (2014). Probing bacterial-fungal interactions at the single cell level. Integr. Biol. (Camb) *6*, 935–945. https://doi.org/10.1039/c4ib00154k.

23. Dijksterhuis, J., and Samson, R.A. (2006). Zygomycetes. In Food Spoilage Microorganisms, C.d.W. Blackburn, ed. (Woodhead Publishing), pp. 415–436. https://doi.org/10.1533/9781845691417.4.415.

24. Fricker, M.D., Tlalka, M., Bebber, D., Takagi, S., Watkinson, S.C., and Darrah, P.R. (2007). Fourier-based spatial mapping of oscillatory phenomena in fungi. Fungal Genet. Biol. *44*, 1077–1084. https://doi.org/10.1016/j.fgb.2007.02.012.

25. Stiefel, P., Schmidt-Emrich, S., Maniura-Weber, K., and Ren, Q. (2015). Critical aspects of using bacterial cell viability assays with the fluorophores SYTO9 and propidium iodide. BMC Microbiol. *15*, 36. https://doi.org/10.1186/s12866-015-0376-x.

26. Moore-Landecker, E. (2008). Zygomycota and glomeromycota. In Encyclopedia of Life Sciences (ELS) (John Wiley & Sons, Ltd.). https://doi.org/10.1002/9780470015902.a0000381.pub2.

27. Rosenberg, M., Azevedo, N.F., and Ivask, A. (2019). Propidium iodide staining underestimates viability of adherent bacterial cells. Sci. Rep. *9*, 6483. https://doi.org/10.1038/s41598-019-42906-3.

28. Uzum, Z., Silipo, A., Lackner, G., De Felice, A., Molinaro, A., and Hertweck, C. (2015). Structure, genetics and function of an exopolysaccharide produced by a bacterium living within fungal hyphae. Chembiochem *16*, 387–392. https://doi.org/10.1002/cbic.201402488.

29. Bierne, H., and Cossart, P. (2012). When bacteria target the nucleus: the emerging family of nucleomodulins. Cell. Microbiol. *14*, 622–633. https://doi.org/10.1111/j.1462-5822.2012.01758.x.

30. Vlisidou, I., Hapeshi, A., Healey, J.R.J., Smart, K., Yang, G., and Waterfield, N.R. (2019). The *Photorhabdus asymbiotica* virulence cassettes deliver protein effectors directly into target eukaryotic cells. eLife *8*, e46259. https://doi.org/10.7554/eLife.46259.

31. Boch, J., Scholze, H., Schornack, S., Landgraf, A., Hahn, S., Kay, S., Lahaye, T., Nickstadt, A., and Bonas, U. (2009). Breaking the code of DNA binding specificity of TAL-type III effectors. Science *326*, 1509–1512. https://doi.org/10.1126/science.1178811.

32. Kay, S., and Bonas, U. (2009). How *Xanthomonas* type III effectors manipulate the host plant. Curr. Opin. Microbiol. *12*, 37–43. https://doi.org/10.1016/j.mib.2008.12.006.

33. de Lange, O., Schreiber, T., Schandry, N., Radeck, J., Braun, K.H., Koszinowski, J., Heuer, H., Strauß, A., and Lahaye, T. (2013). Breaking the DNA-binding code of *Ralstonia solanacearum* TAL effectors provides new possibilities to generate plant resistance genes against bacterial wilt disease. New Phytol. *199*, 773–786. https://doi.org/10.1111/nph.12324.

34. Perez-Quintero, A.L., and Szurek, B. (2019). A decade decoded: spies and hackers in the history of TAL effectors research. Annu. Rev. Phytopathol. *57*, 459–481. https://doi.org/10.1146/annurev-phyto-082718-100026.

35. Stella, S., Molina, R., Bertonatti, C., Juillerrat, A., and Montoya, G. (2014). Expression, purification, crystallization and preliminary X-ray diffraction analysis of the novel modular DNA-binding protein BurrH in its apo form and in complex with its target DNA. Acta Crystallogr. F Struct. Biol. Commun. *70*, 87–91. https://doi.org/10.1107/S2053230X13033037.

36. Schmieder, S.S., Stanley, C.E., Rzepiela, A., van Swaay, D., Sabotič, J., Nørrelykke, S.F., deMello, A.J., Aebi, M., and Künzler, M. (2019). Bidirectional propagation of signals and nutrients in fungal networks via specialized hyphae. Curr. Biol. *29*, 217–228.e4. https://doi.org/10.1016/j.cub.2018.11.058.

37. Hickey, P.C., Jacobson, D., Read, N.D., and Glass, N.L. (2002). Live-cell imaging of vegetative hyphal fusion in Neurospora crassa. Fungal Genet. Biol. *37*, 109–119. https://doi.org/10.1016/s1087-1845(02)00035-x.

38. Desirò, A., Salvioli, A., Ngonkeu, E.L., Mondo, S.J., Epis, S., Faccio, A., Kaech, A., Pawlowska, T.E., and Bonfante, P. (2014). Detection of a novel intracellular microbiome hosted in arbuscular mycorrhizal fungi. ISME J. *8*, 257–270. https://doi.org/10.1038/ismej.2013.151.

39. Kohlmeier, S., Smits, T.H., Ford, R.M., Keel, C., Harms, H., and Wick, L.Y. (2005). Taking the fungal highway: mobilization of pollutant-degrading bacteria by fungi. Environ. Sci. Technol. *39*, 4640–4646. https://doi.org/10.1021/es047979z.

40. Simon, A., Hervé, V., Al-Dourobi, A., Verrecchia, E., and Junier, P. (2017). An *in situ* inventory of fungi and their associated migrating bacteria in forest soils using fungal highway columns. FEMS Microbiol. Ecol. *93*. https://doi.org/10.1093/femsec/fiw217.

41. Chomicki, G., Werner, G.D.A., West, S.A., and Kiers, E.T. (2020). Compartmentalization drives the evolution of symbiotic cooperation. Philos. Trans. R. Soc. Lond. B Biol. Sci. *375*, 20190602. https://doi.org/10.1098/rstb.2019.0602.

42. Limpens, E., and Geurts, R. (2014). Plant-driven genome selection of arbuscular mycorrhizal fungi. Mol. Plant Pathol. *15*, 531–534. https://doi.org/10.1111/mpp.12149.

43. Lackner, G., Moebius, N., Partida-Martinez, L., and Hertweck, C. (2011). Complete genome sequence of *Burkholderia rhizoxinica*, an endosymbiont of *Rhizopus microsporus*. J. Bacteriol. *193*, 783–784. https://doi.org/10.1128/JB.01318-10.

44. Römer, P., Hahn, S., Jordan, T., Strauss, T., Bonas, U., and Lahaye, T. (2007). Plant pathogen recognition mediated by promoter activation of the pepper Bs3 resistance gene. Science *318*, 645–648. https://doi.org/10.1126/science.1144958.

45. Paoletti, M. (2016). Vegetative incompatibility in fungi: from recognition to cell death, whatever does the trick. Fungal Biol. Rev. *30*, 152–162. https://doi.org/10.1016/j.fbr.2016.08.002.

46. Jacobson, D.J., Beurkens, K., and Klomparens, K.L. (1998). Microscopic and ultrastructural examination of vegetative Incompatibility in partial diploids heterozygous at het loci in *Neurospora crassa*. Fungal Genet. Biol. *23*, 45–56. https://doi.org/10.1006/fgbi.1997.1020.

47. Verdier, V., Triplett, L.R., Hummel, A.W., Corral, R., Cernadas, R.A., Schmidt, C.L., Bogdanove, A.J., and Leach, J.E. (2012). Transcription activator-like (TAL) effectors targeting OsSWEET genes enhance virulence on diverse rice (*Oryza sativa*) varieties when expressed individually in a TAL effector-deficient strain of *Xanthomonas oryzae*. New Phytol. *196*, 1197–1207. https://doi.org/10.1111/j.1469-8137.2012.04367.x.

48. Lackner, G., Möbius, N., Scherlach, K., Partida-Martinez, L.P., Winkler, R., Schmitt, I., and Hertweck, C. (2009). Global distribution and evolution of a toxinogenic *Burkholderia-Rhizopus* symbiosis. Appl. Environ. Microbiol. *75*, 2982–2986. https://doi.org/10.1128/AEM.01765-08.

49. Schmitt, I., Partida-Martinez, L.P., Winkler, R., Voigt, K., Einax, E., Dölz, F., Telle, S., Wöstemeyer, J., and Hertweck, C. (2008). Evolution of host resistance in a toxin-producing bacterial-fungal alliance. ISME J. *2*, 632–641. https://doi.org/10.1038/ismej.2008.19.

50. Pérez-Brocal, V., Latorre, A., and Moya, A. (2013). Symbionts and pathogens: what is the difference? In Between Pathogenicity and Commensalism, U. Dobrindt, J.H. Hacker, and C. Svanborg, eds. (Springer), pp. 215–243. https://doi.org/10.1007/82_2011_190.

51. Schindelin, J., Arganda-Carreras, I., Frise, E., Kaynig, V., Longair, M., Pietzsch, T., Preibisch, S., Rueden, C., Saalfeld, S., Schmid, B., et al. (2012). Fiji: an open-source platform for biological-image analysis. Nat. Methods *9*, 676–682. https://doi.org/10.1038/nmeth.2019.

52. Scherlach, K., Partida-Martinez, L.P., Dahse, H.M., and Hertweck, C. (2006). Antimitotic rhizoxin derivatives from a cultured bacterial endosymbiont of the rice pathogenic fungus *Rhizopus microsporus*. J. Am. Chem. Soc. *128*, 11529–11536. https://doi.org/10.1021/ja062953o.

STAR★METHODS

KEY RESOURCES TABLE

REAGENT or RESOURCE	SOURCE	IDENTIFIER
Bacterial and virus strains		
Mycetohabitans rhizoxinica	This study	HKI-454
Electrocompetent Escherichia coli TOP10	Invitrogen	CAT#C404052
Chemicals, peptides, and recombinant proteins		
Potato Dextrose Agar	Becton, Dickinson & Co.	CAT#213400
Glycerol	Roth	CAT#6967.1
Yeast Extract	Becton, Dickinson & Co.	CAT#288620
K_2HPO_4	Roth	CAT#P749.2
KH_2PO_4	Roth	CAT#3904.1
C_6H_7NaO	Roth	CAT#HN13.3
$(NH_4)_2SO_4$	Roth	CAT#9212.1
Mg_2SO_4	Roth	CAT#P027.1
Standard Nutrient Agar I	Merck	CAT#1.03864.0500
Phusion® High-Fidelity PCR Master Mx	New England Biolabs	CAT#M0530L
Apramycin	Sigma	CAT#A2024
SpeI	New England Biolabs	CAT#R3133L
KpnI	New England Biolabs	CAT#R3142L
OneTAQ® Quick-Load® 2x Master Mix	New England Biolabs	CAT#M0486L
Ethidium bromide	New England Biolabs	CAT#E1510
NdeI	New England Biolabs	CAT#R0111L
AflII	New England Biolabs	CAT#R0520L
BstBI	New England Biolabs	CAT#R0519L
Chloramphenicol	Roth	CAT#3886.1
Potato Dextrose Broth	Becton, Dickinson & Co.	CAT#254920
NaCl	Roth	CAT#3957.1
SYTO™ 9	Invitrogen	CAT#S34854
LIVE/DEAD™ BacLight™ Bacterial Viability Kit	Invitrogen	CAT#L7012
Propidium iodide	Invitrogen	CAT#P21493
Calcofluor white	Sigma	CAT#18909
GeneRuler™ DNA Ladder Mix	Thermo Scientific	CAT#SM0333
T4 DNA Ligase	New England Biolabs	CAT#M0202L
Ciprofloxacin	Sigma	CAT#17850
Critical commercial assays		
Monarch® DNA Gel Extraction Kit	New England Biolabs	CAT#T1020L
NEBuilder® HiFi DNA Assembly Cloning Kit	New England Biolabs	CAT#E2621L
MasterPure™ DNA Purification Kit	Biozym	CAT#160502
Monarch® Plasmid Miniprep Kit	New England Biolabs	CAT#T1010L
Experimental models: Organisms/strains		
Rhizopus microsporus	Jena Microbial Resource Collection	ATCC 62417
Oligonucleotides		
See Data S6 for a list of oligonucleotides		N/A
Recombinant DNA		
Plasmid pZU17	This paper	N/A
Plasmid pBBR-*mtaI1*	This paper	N/A
Plasmid pBBR∅	This paper	N/A

(*Continued on next page*)

Continued		
REAGENT or RESOURCE	SOURCE	IDENTIFIER
Plasmid pGL42	Lackner et al.[16,43]	N/A
Software and algorithms		
Zen Blue	Zeiss	N/A
Zen Black	Zeiss	N/A
Fiji	Schindelin et al.[51]	N/A
GraphPad Prism 9.0	GraphPad Software	N/A
Other		
M. rhizoxinica genome	Lackner et al.[16,43]	Genbank Accession #GCA_000198775.1
NanoDrop™ One	Thermo Scientific	N/A
Eporator Electroporator	Eppendorf	N/A
Quantum ST5 Xpress Gel Imager	Vilber Lourmat	N/A
Bacterial-Fungal-Interaction devicesDevices	This paper	N/A
CASY Cell Counter	OMNI Life Science	N/A
Fluorescence Spinning Disc Microscope	Zeiss	Axio Observer platform with Cell Observer SD
Confocal Laser Scanning Microscope	Zeiss	LSM 710
Fluorescence Widefield Microscope	Zeiss	Elyra7

RESOURCE AVAILABILITY

Lead contact

Further information and requests for resources and reagents should be directed to and will be fulfilled by the lead contact, Christian Hertweck (Christian.Hertweck@leibniz-hki.de).

Materials availability

This study did not generate new unique reagents.

Data and code availability

- This paper analyzes existing, publicly available data. The accession numbers for the datasets are listed in the key resources table.
- Microscopy data reported in this paper will be shared by the lead contact upon request.

EXPERIMENTAL MODEL AND SUBJECT DETAILS

The fungal strain *Rhizopus microsporus* ATCC62417 harboring the endobacteria *Mycetohabitans rhizoxinica* was used in this study.[48] Endobacteria from *R. microsporus* ATCC62417 were eliminated by continuous antibiotic treatment[10] and the apo-symbiotic fungal strain was named ATCC62417/S. Absence of endobacteria was confirmed by fluorescence microscopy and an absence of rhizoxin extracts of the fungal mycelium.[52] Both *R. microsporus* strains (ATCC62417 and ATCC62417/S) were cultivated on Potato Dextrose Agar (PDA; Becton, Dickinson & Company, Sparks, MD, USA) at 30 °C. Bacterial endosymbionts were isolated from *R. microsporus* mycelium as previously reported.[10] Axenic cultures of *M. rhizoxinica* were grown at 30 °C in MGY M9 medium (10 g/L glycerol, 1.25 g/L yeast extract, M9 salts: 40 mM K_2HPO_4, 14 mM KH_2PO_4, 2.2 mM $C_6H_7NaO_7$, 7.5 mM $(NH_4)_2SO_4$, and 0.8 mM Mg_2SO_4) or Standard I Nutrient Agar (Merck, Darmstadt, Germany) supplemented with 1% glycerol.

METHOD DETAILS

Generation of *M. rhizoxinica* Δ*mtal1* strains

To investigate the role of MTAL1 in the symbiosis, the *mtal1* gene (RBRH_01844) was deleted using a double crossover strategy as previously described.[16]

Using a proofreading polymerase, the upstream and downstream regions of the gene of interest were amplified. Primers were designed to contain 20 bp overlap with the gene of interest as well as a 20 bp overlap with an antibiotic resistance cassette (apramycin). The apramycin cassette was amplified from pJI773 using primers carrying the same 20 bp.

The knockout vector pGL42a was used to generate a *M. rhizoxinica* Δ*mtal1*::Apra^R deletion mutant. pGL42a was double-digested with the restriction enzymes SpeI and KpnI (New England Biolabs, Ipswich, MA, USA). The linear vector was gel-purified (Monarch® DNA Gel Extraction Kit, New England Biolabs) and quantified using a NanoDrop™ (Thermo Fisher Scientific).

Equimolar amounts of three PCR products and linear pGL42a were mixed with NEBuilder® 2X Master Mix (NEBuilder® HiFi DNA Assembly Cloning Kit, New England Biolabs) and incubated at 60 °C for 1 hr following the manufacturer's recommendations. The new plasmid pZU17 (Δ*mtal1*) was introduced into *E. coli* by chemical transformation. Transformants were selected on Standard I Nutrient Agar (Merck) supplemented with 50 μg/mL apramycin and 1% glycerol (pZU17).

Competent *M. rhizoxinica* HKI-454 (M1WT) cells were transformed with pZU17 via electroporation. Transformants were grown on standard nutrient agar containing 50 μg/mL of apramycin. Colonies were subsequently passaged onto agar plates containing double selection medium[16] until the correct knockout constructs were observed using colony PCR. Colony PCRs were carried out in 12.0 μL final volumes containing: 5 μL of high-fidelity OneTaq® Quick-Load® 2X Master Mix (New England Biolabs), appropriate forward and reverse control primers (both 0.4 μM, Data S6A), and 5 μL colony suspension. The following thermocycling conditions were used for amplification: 96 °C / 3 min, 1 cycle; 96 °C / 10 s, 58 °C / 15 s, 68 °C / 1 min, 30 cycles; 68 °C / 5 min, 1 cycle; 16 °C / hold. The resulting PCR products were visualized on an agarose gel (Figure S1E). Primers were designed to span the two recombination sites, yielding amplicons A and B in *M. rhizoxinica* Δ*mtal1* strains and amplicons C and D in *M. rhizoxinica* wild type strains (Figures S1A and S1B).

Generation of genetically complemented *M. rhizoxinica* Δ*mtal1* strains

In order to genetically complement the knockout strain *M. rhizoxinica* Δ*mtal1*, genomic DNA from *M. rhizoxinica* (M1WT) was isolated using the MasterPure™ DNA Purification Kit (Biozym Scientific, Hessisch Oldendorf, Germany) following the manufacturer's recommendations. The *mtal1* gene was amplified by PCR with the primer pairs listed in Data S6B using Phusion® High-Fidelity PCR Master Mix with HF Buffer (New England Biolabs). The PCR product was gel-purified with the Monarch DNA Gel Extraction Kit (New England Biolabs). The purified amplicon was cloned into the *Nde*I/*Afl*II restricted pBBR_P$_{s12}$_*gfp* downstream of the promoter P$_{s12}$ with the NEBuilder® 2X Master Mix (NEBuilder® HiFi DNA Assembly Cloning Kit, New England Biolabs), yielding pBBR-*mtal1* (Figure S1D). The reaction mixture was subsequently used to transform chemically competent *E. coli* TOP10 cells (Invitrogen™, One Shot™, Carlsbad, CA, USA).

To generate an empty vector control, pBBR_P$_{s12}$_*gfp* was digested with the restriction enzyme *BstB*I. The resulting linear vector lacking *gfp* was self-circularized using T4 DNA Ligase (New England Biolabs) to yield pBBR∅ and used to transform chemically competent *E. coli* TOP10 cells (Invitrogen™, One Shot™). All plasmids were purified from *E. coli* TOP10 overnight cultures using the Monarch Plasmid Miniprep Kit (New England Biolabs) and verified by restriction digest and Sanger sequencing using the primers *cm^r*_seq_fw and BBR_seq_rv (Data S6B).

The new plasmids (pBBR-*mtal1* or pBBR∅) were introduced into competent *M. rhizoxinica* Δ*mtal1* cells via electroporation. Transformants were grown on standard nutrient agar containing 50 μg/mL chloramphenicol and 50 μg/mL apramycin. Colonies containing the respective plasmids were observed using colony PCR and control primers (Figure S1E; Data S6B).

Inoculation of bacterial-fungal interaction devices with fungus

Bacterial-fungal interaction (BFI) devices were prepared as previously described.[22] Before the BFI devices were inoculated, aposymbiotic (endosymbiont-free) *R. microsporus* ATCC62417/S was sub-cultured on PDA plates for two days at 30 °C. A piece of young, growing mycelium (app. 1 cm^3) was cut from the agar plate and placed upside down in front of the microchannels of a BFI device filled with Potato Dextrose Broth (PDB; Becton, Dickinson & Company). The agar plug was positioned with the growth direction of the fungus facing the microchannels. We paid special attention to the size of the agar plug to minimize variation between experiments. After two days of incubation at 30 °C, the hyphae had grown far enough into the microchannels to perform subsequent reinfection experiments.

Bacterial inoculation into bacterial-fungal interaction devices

Bacterial over-night cultures (500 μL) were harvested in an Eppendorf tube and resuspended in 0.5 mL NaCl (0.85%) containing SYTO9 (5 nM final concentration, Invitrogen). Following incubation in the dark for 5 min, stained cells were washed and resuspended in 0.5 mL PDB medium. Cells were counted using a CASY Cell Counter (OMNI Life Science, Bremen, Germany) and then added to the bacteria inlet of the BFI device (100 μL), which is connected with the microchannels containing the cured fungus (Figures 2A and 2B).

Live-cell imaging of bacterial-fungal interactions

A fluorescence spinning disc microscope (Axio Observer microscope-platform equipped with Cell Observer SD, Zeiss, Oberkochen, Germany) was used to visualize BFIs at 0 h, 24 h, and 48 h after bacterial inoculation. For each time point, 16 images were taken at random positions of the microchannels, including both ends of the BFI device (N = 16 technical replicates). Bright-field images were captured using a laser intensity of 7.1 V and an exposure time of 100 ms. Images of bacterial cells (*M. rhizoxinica* wild type, *M. rhizoxinica* Δ*mtal1, M. rhizoxinica* Δ*mtal1* pBBR∅, *M. rhizoxinica* Δ*mtal1* pBBR-*mtal1, M. rhizoxinica* Δ*sctT, M. rhizoxinica* Δ*sctC, and M. rhizoxinica* Δ*rhiG*), stained with SYTO9, were captured at 485/498 nm with an exposure time of 100 ms. As a reference, wild-type *R. microsporus* ATCC62417, naturally containing endosymbionts, was also analyzed, without additional bacterial cultures being added through the inlet. Each reinfection experiment was performed three times independently (N = 3 biological replicates).

Imaging of bacterial survival inside of bacterial-fungal interaction devices

To test the bacterial survival rate in BFI devices, cells were stained with LIVE/DEAD BacLight fluorescent dyes (Invitrogen) after 72 h of bacterial-fungal co-incubation. The fungal cell wall was counter-stained with calcofluor white (Sigma-Aldrich, St. Louis, MI, USA). To stain fungal and bacterial cells inside the BFI device, the PDB medium was removed through the bacteria inlet and replaced with 100 μL staining solution (10 nM SYTO9, 60 nM propidium iodide (Invitrogen), 1 μM calcofluor white). Fluid replacement was repeated three times, before the devices were incubated in the dark for 15 min. Following staining, fluorescent dyes were replaced with PDB medium by flushing the devices four times. Fluorescence microscopy was carried out using a fluorescence spinning disc microscope (Axio Observer microscope-platform equipped with Cell Observer SD, Zeiss). Images of living bacterial cells were captured at 485/498 nm, dead bacterial cells were captured at 493/636 nm, and the fungal cell wall was captured at 380/475 nm using the Zeiss-Zen software.

Quantification of bacterial cells inside of fungal hyphae

Fluorescent images, containing spatial calibration meta data, were imported to Fiji[51] and the same spatial scale was applied to all images using the global scale function. Prior to image analyses, all images were converted to 16-bit gray-scale, which was propagated to all channels (brightfield, 485/498 nm, 493/636 nm). The hyphal area and integrated density (ID; product of area and mean grey value) of all channels were measured using the freehand tool and measuring tool implemented in Fiji. According to the brightfield images, four types of hyphae were defined (Figure 2C) and the number of septa observed was counted. Subsequent calculations and data visualization were carried out using MS Excel and GraphPad Prism 9.0. To correct for background autofluorescence, raw ID values at 0 hours post infection (hpi) were subtracted from raw ID values at 24 hpi and 48 hpi. Corrected ID values were divided by the number of bacterial cells (cells/mL) inoculated in the bacteria inlet and then plotted. The same approach was applied to correct for the number of septa observed. The corrected number of septa was divided by the mycelium area analyzed (in μm).

Imaging of axenic bacterial cultures

To test whether stained bacteria remain detectably stained, axenic *M. rhizoxinica* wild type, *M. rhizoxinica* Δ*mtal1, M. rhizoxinica* Δ*mtal1* pBBR∅ or *M. rhizoxinica* Δ*mtal1* pBBR-*mtal1* were grown at 30 °C in 2 mL MGY M9 medium. When the exponential phase was reached, bacterial cells (1 mL) were stained with 5 nM SYTO9 for 5 min. Fluorescence microscopy was carried out using a fluorescence wide-field microscope (ELYRA 7, Zeiss). Images of bacterial cells were captured at 485/498 nm using the Zeiss-Zen software. Stained cells were centrifuged, the cell pellets were resuspended in 2 mL fresh MGY M9 medium, and the bacterial cultures were incubated at 30 °C. After 24 h of incubation, 20 μL of cells were used for fluorescence imaging at 485/498 nm. Sub-cultures (1 mL) of the 24-hour-old cultures were centrifuged, the cell pellets were resuspended in 2 mL fresh MGY M9 medium, and the bacterial cultures were incubated at 30 °C. After 24 h of incubation, 20 μL of the 48-hour-old cultures were used for fluorescence imaging at 485/498 nm.

Imaging of fungal septa

Fungal hyphae were harvested from one-week old bacterial-fungal co-cultures, stained with 5 nM SYTO9 and 1 μM calcofluor white, and fixed on glass slides. Fluorescent microscopy was performed using a confocal laser scanning microscope (LSM 710 equipped with a Cell Observer SD, Zeiss). Images of bacterial cells were captured at 485/498 nm and the fungal cell wall was captured at 380/475 nm using the Zeiss-Zen software.

QUANTIFICATION AND STATISTICAL ANALYSIS

Raw data from reinfection experiments and bacterial survival experiments were processed with MS Excel. GraphPad Prism 9.0 was used for statistical analysis and graphing. One-way analysis of variance (ANOVA) was used to study the relationship between different *M. rhizoxinica* strains (*M. rhizoxinica* wild type, *M. rhizoxinica* Δ*mtal1, M. rhizoxinica* Δ*mtal1* control, or *M. rhizoxinica* Δ*mtal1* pBBR-*mtal1*) and fungal physiology (e.g. mycelium area, reinfection efficiency, septation rate, bacterial survival) following fungal reinfection using the Tukey HSD test function. P-values with $p<0.05$ were considered statistically significant. The Brown-Forsythe test was used to test for equal variance and a p value with <0.05 was considered significant.

Current Biology, Volume *33*

Supplemental Information

Transcription activator-like effector protects bacterial endosymbionts from entrapment within fungal hyphae

Ingrid Richter, Philipp Wein, Zerrin Uzum, Claire E. Stanley, Jana Krabbe, Evelyn M. Molloy, Nadine Moebius, Iuliia Ferling, Falk Hillmann, and Christian Hertweck

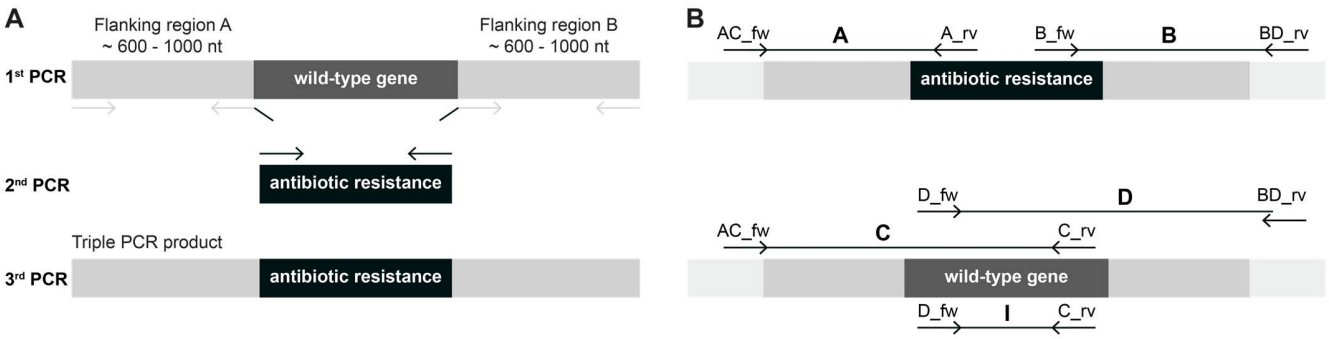
A
Flanking region A
~ 600 - 1000 nt
Flanking region B
~ 600 - 1000 nt
1st PCR
wild-type gene
2nd PCR
antibiotic resistance
Triple PCR product
3rd PCR
antibiotic resistance
B
AC_fw
A
A_rv
B_fw
B
BD_rv
antibiotic resistance
D_fw
D
BD_rv
AC_fw
C
C_rv
wild-type gene
D_fw
I
C_rv

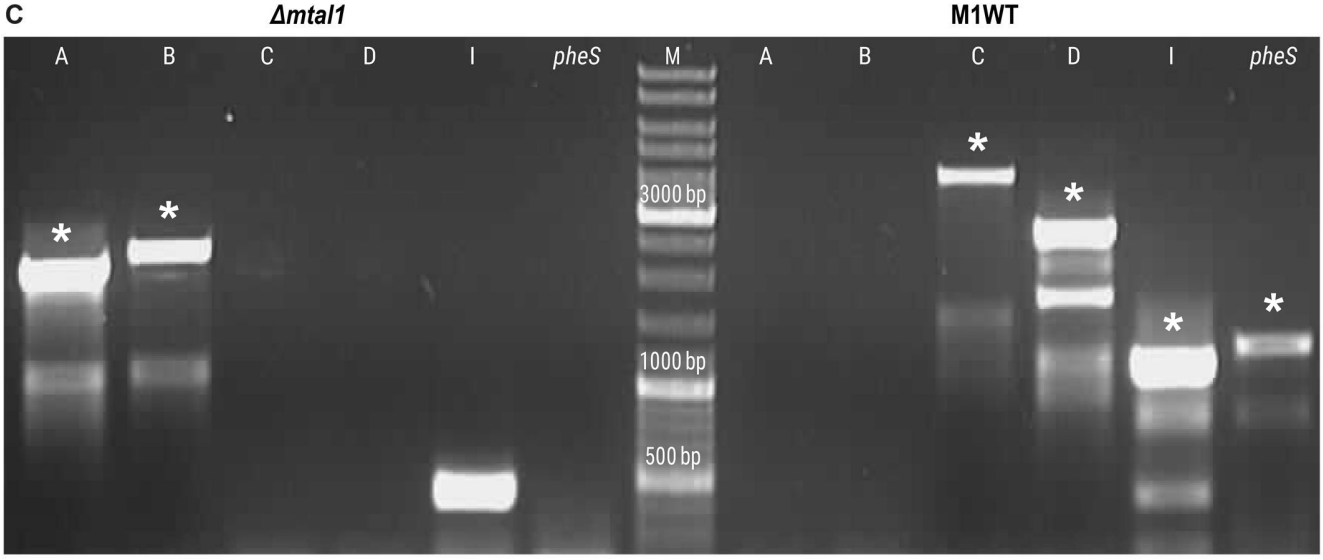
C
Δmtal1
M1WT
A
B
C
D
I
pheS
M
3000 bp
1000 bp
500 bp

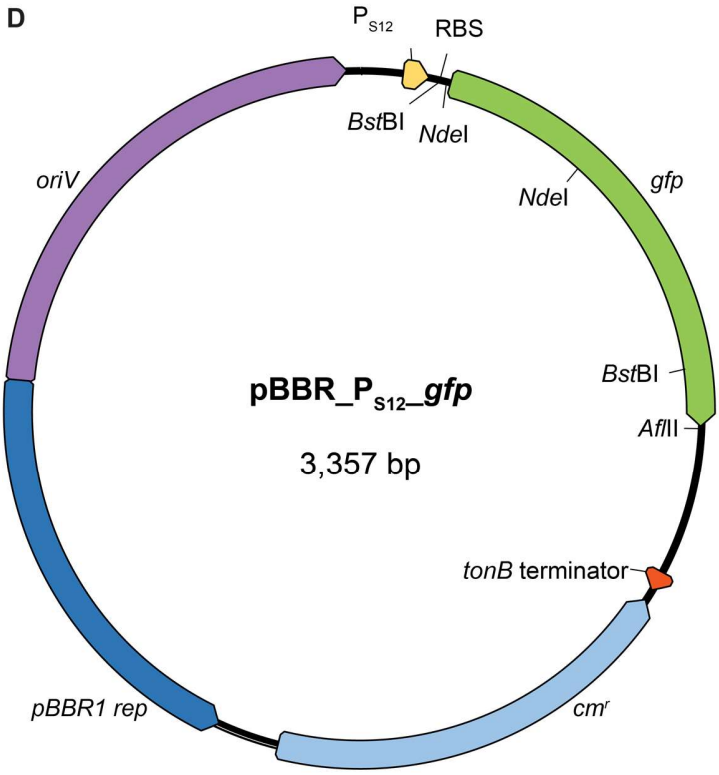
D
P S12
RBS
BstBI
NdeI
oriV
NdeI
gfp
BstBI
AflII
pBBR_P S12_gfp
3,357 bp
tonB terminator
pBBR1 rep
cmr

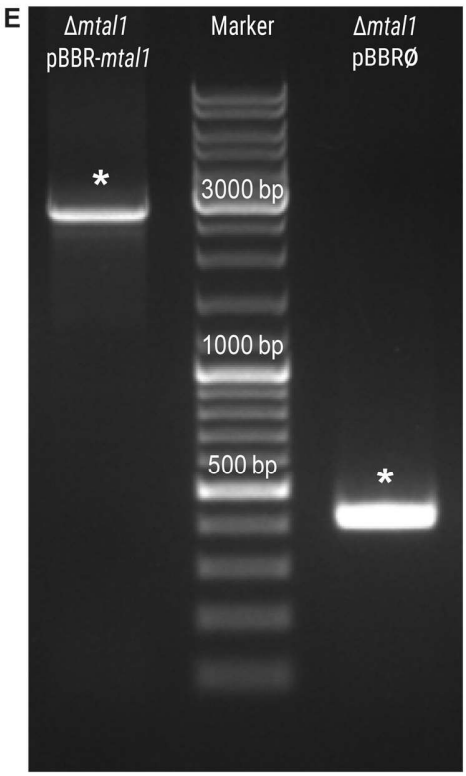
E
Δmtal1
pBBR-mtal1
Marker
Δmtal1
pBBRØ
3000 bp
1000 bp
500 bp

Figure S1. Generation and confirmation of *Mycetohabitans rhizoxinica* transcription-activator like effector (MTAL) knock out and complemented strains (related to STAR methods).
(A) Schematic representation of the construction of knockout vectors.
(B) Schematic representation of the confirmation of the successful gene inactivation. The PCR products of the knockout strain correspond to amplicons A and B; whereas products C and D are amplified from the wild type. The knockout strains were checked for the absence of contaminating *M. rhizoxinica* wild type (M1WT) by amplifying an internal fragment (amplicon I) form the wild type gene of interest. The removal of the knockout vector was confirmed by amplification of the counter selection marker gene *pheS* (amplicons pheS).
(C) The *mtal1* gene was deleted to generate *M. rhizoxinica* Δ*mtal1*. PCR products were obtained from genomic wild type and Δ*mtal1* DNA using control primers listed in Data S6A. Bands corresponding to the expected size are indicated by asterisks (*).
(D) Schematic of the vector used to generate complementation plasmids.
(E) Confirmation of complemented *M. rhizoxinica* Δ*mtal1* (Δ*mtal1* pBBR-*mtal1*) by colony PCR. *M. rhizoxinica* Δ*mtal1* was also transformed with an empty control plasmid as negative control generating *M. rhizoxinica* Δ*mtal1* pBBR∅. PCR products were amplified using control primers listed in Data S6B. Bands corresponding to the expected size are indicated by asterisks (*).

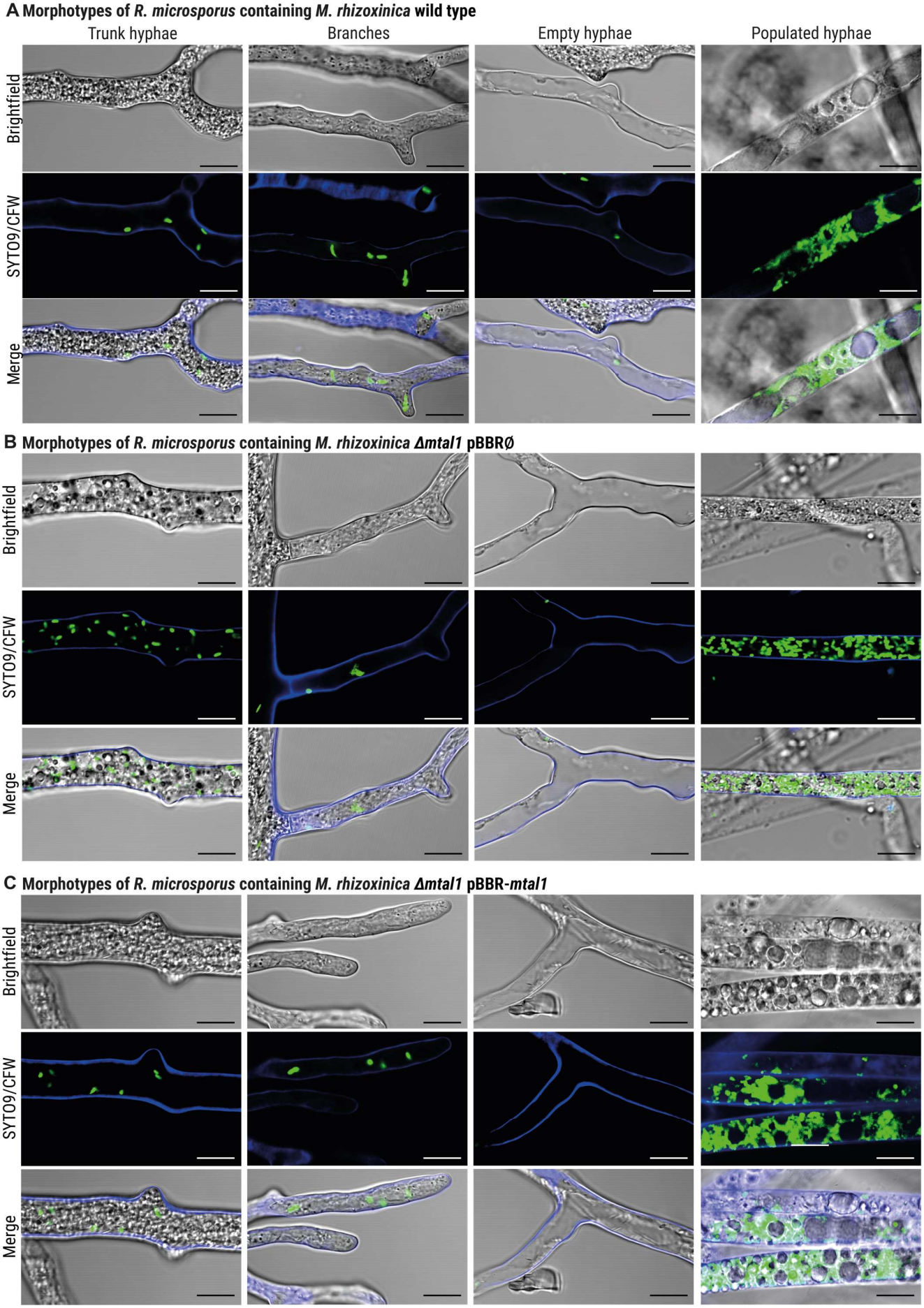
A Morphotypes of R. microsporus containing M. rhizoxinica wild type
Trunk hyphae
Branches
Empty hyphae
Populated hyphae
Brightfield
SYTO9/CFW
Merge
B Morphotypes of R. microsporus containing M. rhizoxinica Δmtal1 pBBRØ
Brightfield
SYTO9/CFW
Merge
C Morphotypes of R. microsporus containing M. rhizoxinica Δmtal1 pBBR-mtal1
Brightfield
SYTO9/CFW
Merge

Figure S2. Phenotypic observations of *Rhizopus microsporus* co-cultivated with SYTO9-stained *Mycetohabitans rhizoxinica* strains in bacterial-fungal interaction (BFI) devices (related to Figure 2C).
(A) Microscopic images of *R. microsporus* (stained with calcofluor white) co-cultivated with *M. rhizoxinica* wild type depicting four types of hyphae. Scale bars: 10 µm.
(B) Microscopic images of *R. microsporus* (stained with calcofluor white) co-cultivated with *M. rhizoxinica* Δ*mtal1* control (Δ*mtal1* pBBRØ) depicting four types of hyphae. Scale bars: 10 µm.
(C) Microscopic images of *R. microsporus* (stained with calcofluor white) co-cultivated with complemented *M. rhizoxinica* Δ*mtal1* (*M. rhizoxinica* Δ*mtal1* pBBR-*mtal1*) depicting four types of hyphae. Scale bars: 10 µm.

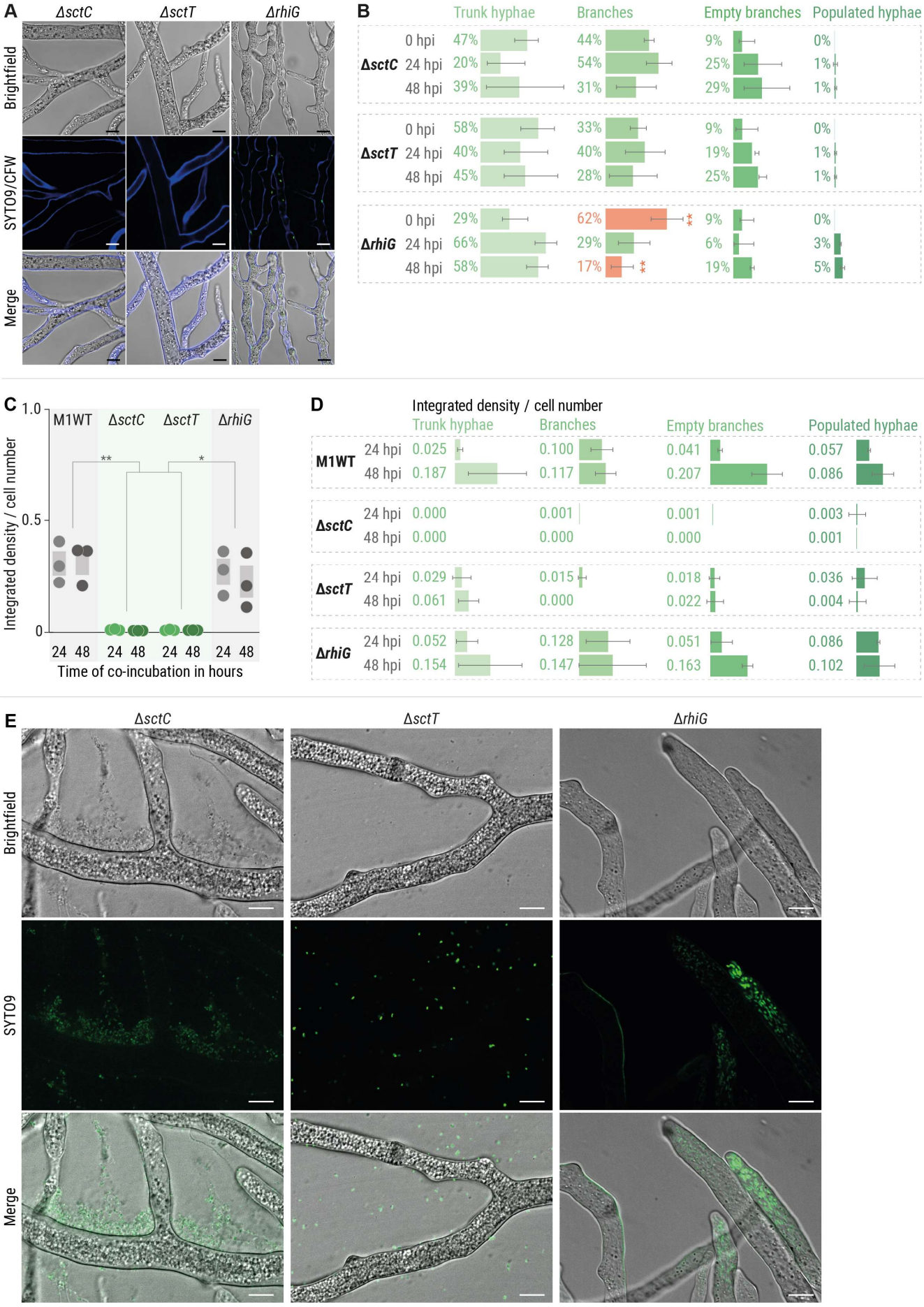
A
ΔsctC
ΔsctT
ΔrhiG
Brightfield
SYTO9/CFW
Merge
B
Trunk hyphae
Branches
Empty branches
Populated hyphae
ΔsctC
0 hpi 47% 44% 9% 0%
24 hpi 20% 54% 25% 1%
48 hpi 39% 31% 29% 1%
ΔsctT
0 hpi 58% 33% 9% 0%
24 hpi 40% 40% 19% 1%
48 hpi 45% 28% 25% 1%
ΔrhiG
0 hpi 29% 62% ** 9% 0%
24 hpi 66% 29% 6% 3%
48 hpi 58% 17% * 19% 5%
C
M1WT
ΔsctC
ΔsctT
ΔrhiG
Integrated density / cell number
1.0
0.5
0
**
*
24 48 24 48 24 48 24 48
Time of co-incubation in hours
D
Integrated density / cell number
Trunk hyphae
Branches
Empty branches
Populated hyphae
M1WT
24 hpi 0.025 0.100 0.041 0.057
48 hpi 0.187 0.117 0.207 0.086
ΔsctC
24 hpi 0.000 0.001 0.001 0.003
48 hpi 0.000 0.000 0.000 0.001
ΔsctT
24 hpi 0.029 0.015 0.018 0.036
48 hpi 0.061 0.000 0.022 0.004
ΔrhiG
24 hpi 0.052 0.128 0.051 0.086
48 hpi 0.154 0.147 0.163 0.102
E
ΔsctC
ΔsctT
ΔrhiG
Brightfield
SYTO9
Merge

Figure S3. Phenotypic observation and quantification of *Rhizopus microsporus* co-cultivated with *Mycetohabitans rhizoxinica* knockout strains in bacterial-fungal interaction (BFI) devices (related to Figures 2C and 2D, Figures 3A and 3B).

(A) Microscopic images of *R. microsporus* (stained with calcofluor white) co-cultivated with *M. rhizoxinica* type 3 secretion system knockout strains (*M. rhizoxinica* Δ*sctC* or *M. rhizoxinica* Δ*sctT*), or a rhizoxin-deficient strain (*M. rhizoxinica* Δ*rhiG*). Bacterial strains were stained with SYTO9 prior to co-incubation. Scale bars: 10 µm.

(B) The fungal mycelium area (as a percentage) of each type of hyphae was measured over a 48-hour time period of co-incubation in BFI devices. At time point 0, cultures of *M. rhizoxinica* Δ*sctC*, *M. rhizoxinica* Δ*sctT*, or *M. rhizoxinica* Δ*rhiG* were stained with SYTO9, individually added to the inlet, and co-incubated with apo-symbiotic *R. microsporus*. Images were taken at the time of infection (0 hours post infection; hpi), as well as 24 and 48 hpi. N = 3 biological replicates ± SEM (Data S1E – S1H).

(C) Apo-symbiotic *R. microsporus* was co-incubated with SYTO9-stained *M. rhizoxinica* wild type (M1WT), T3SS-deficient *M. rhizoxinica* (*M. rhizoxinica* Δ*sctC* or *M. rhizoxinica* Δ*sctT*), or rhizoxin-deficient *M. rhizoxinica* (*M. rhizoxinica* Δ*rhiG*) for 48 hours. Following fluorescence microscopy at 485/498 nm, the integrated density per bacterial cell number was calculated for both measurements (24 and 48 hours post infection; hpi) using Fiji. Dots represent three independent replicates (N = 3 biological replicates) ± SEM (grey bars). One-way ANOVA with Tukey's multiple comparison test (**p<0.05*, ***p<0.002*, SI Appendix, Data S2E – S2H).

(D) The integrated density per cell number was measured for each individual type of hyphae following reinfection with *M. rhizoxinica* wild type (M1WT), *M. rhizoxinica* Δ*sctC*, *M. rhizoxinica* Δ*sctT*, or *M. rhizoxinica* Δ*rhiG*. N = 3 biological replicates ± SEM. One-way ANOVA with Tukey's multiple comparison test (Data S3E – S3H).

(E) Fluorescence microscopy images of *R. microsporus* co-incubated with *M. rhizoxinica* Δ*sctC*, *M. rhizoxinica* Δ*sctT*, or *M. rhizoxinica* Δ*rhiG*. T3SS-deficient *M. rhizoxinica* are unable to reinfect *R. microsporus*, while fungal reinfection by rhizoxin-deficient *M. rhizoxinica* is similar to wild-type *M. rhizoxinica*. Scale bars: 10 µm.

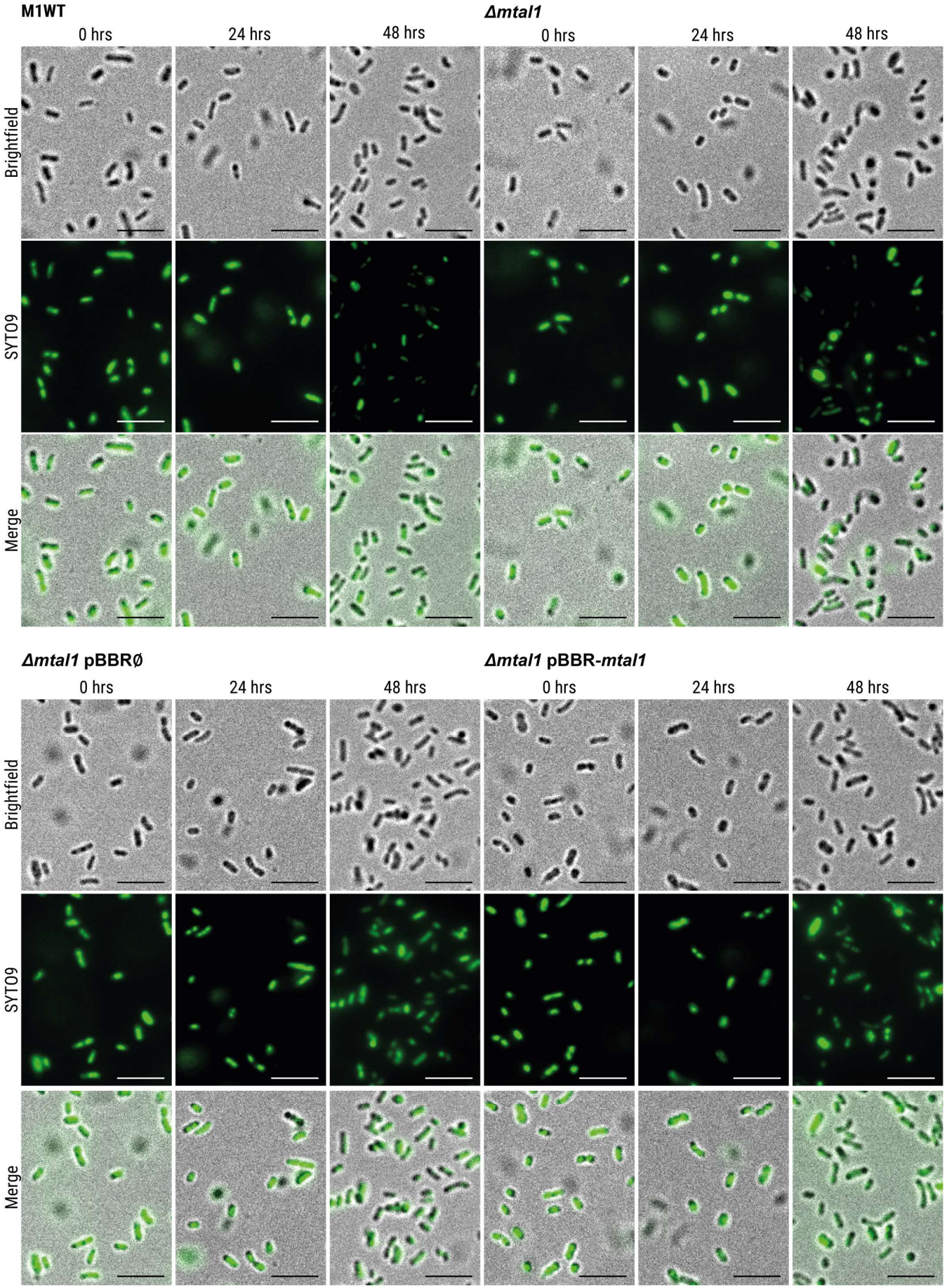
M1WT
Δmtal1
0 hrs
24 hrs
48 hrs
0 hrs
24 hrs
48 hrs
Brightfield
SYTO9
Merge
Δmtal1 pBBRØ
Δmtal1 pBBR-mtal1
0 hrs
24 hrs
48 hrs
0 hrs
24 hrs
48 hrs
Brightfield
SYTO9
Merge

Figure S4. Imaging of axenic SYTO9-stained *Mycetohabitans rhizoxinica* cells over 48 hours of growth (related to Figure 3A). To test whether SYTO9-stained bacteria remain detectably stained, axenic *M. rhizoxinica* wild type, *M. rhizoxinica* Δ*mtal1, M. rhizoxinica* Δ*mtal1* pBBR∅ or *M. rhizoxinica* Δ*mtal1* pBBR-*mtal1* were imaged after 0, 24, and 48 hrs of incubation. Scale bars: 5 µm.

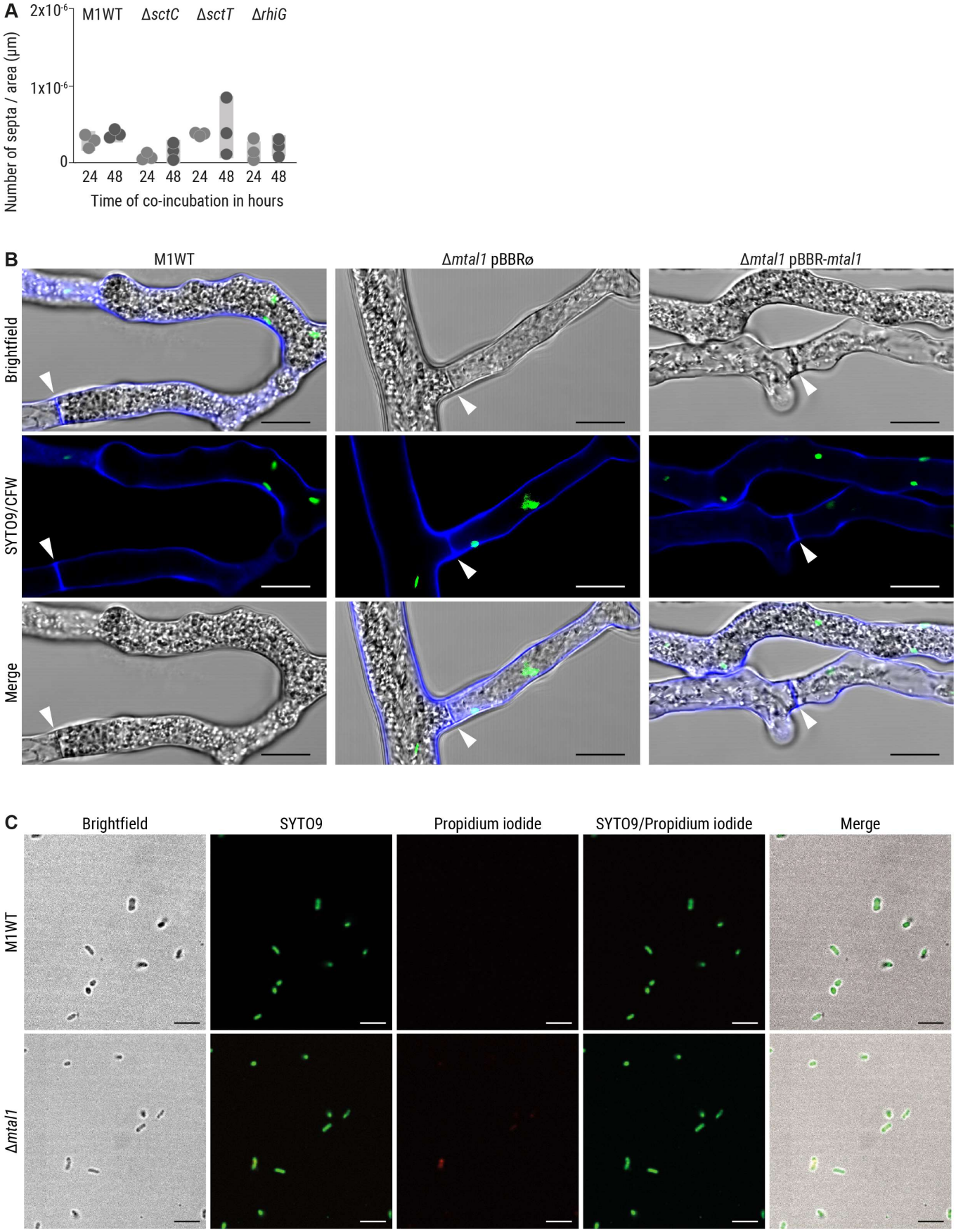
A
2x10-6
1x10-6
0
M1WT
ΔsctC
ΔsctT
ΔrhiG
Number of septa / area (µm)
24 48 24 48 24 48 24 48
Time of co-incubation in hours
B
M1WT
Δmtal1 pBBRø
Δmtal1 pBBR-mtal1
Brightfield
SYTO9/CFW
Merge
C
Brightfield
SYTO9
Propidium iodide
SYTO9/Propidium iodide
Merge
M1WT
Δmtal1

Figure S5. Septa formation in *Rhizopus microsporus* following co-incubation with *Mycetohabitans rhizoxinica* strains (related to Figure 4B and Figure 5A).
(A) The number of septa per area (in µm) was calculated for *R. microsporus* containing either *M. rhizoxinica* wild-type (M1WT), T3SS-deficient *M. rhizoxinica* (*M. rhizoxinica* Δ*sctC* or *M. rhizoxinica* Δ*sctT*), or rhizoxin-deficient *M. rhizoxinica* (*M. rhizoxinica* Δ*rhiG*). Dots represent three independent replicates (N = 3 biological replicates ± SEM). One-way ANOVA with Tukey's multiple comparison test (Data S4E – S4H).
(B) Fluorescence microscopy images showing the formation of septa (blue) in *R. microsporus* following co-incubation with *M. rhizoxinica* wild-type (M1WT), *M. rhizoxinica* Δ*mtal1* pBBRØ, or *M. rhizoxinica* Δ*mtal1* pBBR-*mtal1* (green). Scale bars: 10 µm.
(C) The majority of axenic wild-type *Mycetohabitans rhizoxinica* (M1WT) and *Mycetohabitans* transcription-activator like effector 1 (MTAL1) mutant strains are alive. M1WT and MTAL1 mutant strains (*Δmtal1*) were visualized with LIVE/DEAD BacLight fluorescent dyes. Green fluorescence (SYTO9) indicates that bacteria are alive, while red fluorescence (propidium iodide) is indicative of dead bacteria. Scale bars: 5 µm.